THE PENNSYLVANIA STATE UNIVERSITY
SCHREYER HONORS COLLEGE

DEPARTMENT OF MECHANICAL AND NUCLEAR ENGINEERING

MODELING COMPLIANT MECHANISM FLEXURE HINGES FOR FLAPPING WING NANO AIR VEHICLES

PETER ALAN KOFFLER
FALL 2012

A thesis
submitted in partial fulfillment
of the requirements
for a baccalaureate degree
in Mechanical Engineering
with honors in Mechanical Engineering

Reviewed and approved* by the following:

Christopher D. Rahn
Professor of Mechanical Engineering
Thesis Supervisor

H. Joseph Sommer III
Professor of Mechanical Engineering
Honors Adviser

* Signatures are on file in the Schreyer Honors College.

Abstract

The piezoelectrically actuated flapping wing nano air vehicle at the center of this analysis was developed by Dr. Kiron Mateti for a PhD Thesis supervised by Dr. Chris Rahn over the past five years [1]. The design of the Eristalis flapping wing is unique for its single material construction. Small scale assembly procedures common in other nano air vehicles were eliminated by etching the required wing geometry from a single sheet of SUEX epoxy photoresist material. The resulting wing utilizes compliant mechanism flexure hinges instead of more conventional multi-part hinges to transfer loads. The design was tested extensively by Dr. Mateti to measure the thrust produced by flapping for different wing and hinge geometries. However, a common occurance during the wing testing was the failure of the complaint beam hinges. This thesis focuses on determining the stresses in the compliant flexure hinges using both beam theory and ANSYS Finite Element Analysis software. Identical displacement and force loads will be prescribed to hinge models of complexity ranging from 2D beam to 3D solid elements. Both static and dynamic operation of the wing will be considered. The results of various stress analysis techniques will be compared to help future flexure hinge designers model stresses by the simplest means possible while still achieving sufficient accuracy.

Table of Contents

List of Figures

List of Tables

Introduction

The design, manufacture, dynamic system modeling, and experimental testing of the Eristalis wing and other air vehicles are described in Dr. Kiron Mateti's PhD Dissertation titled, "Flapping Wing Mechanisms for Pico Air Vehicles Using Piezoelectric Actuators." [1] The analysis in this thesis will focus on the flexure hinges in the Eristalis wing design, named after a genus of hovering flies. The Eristalis wing can be seen in the undeformed position in Figure 1.

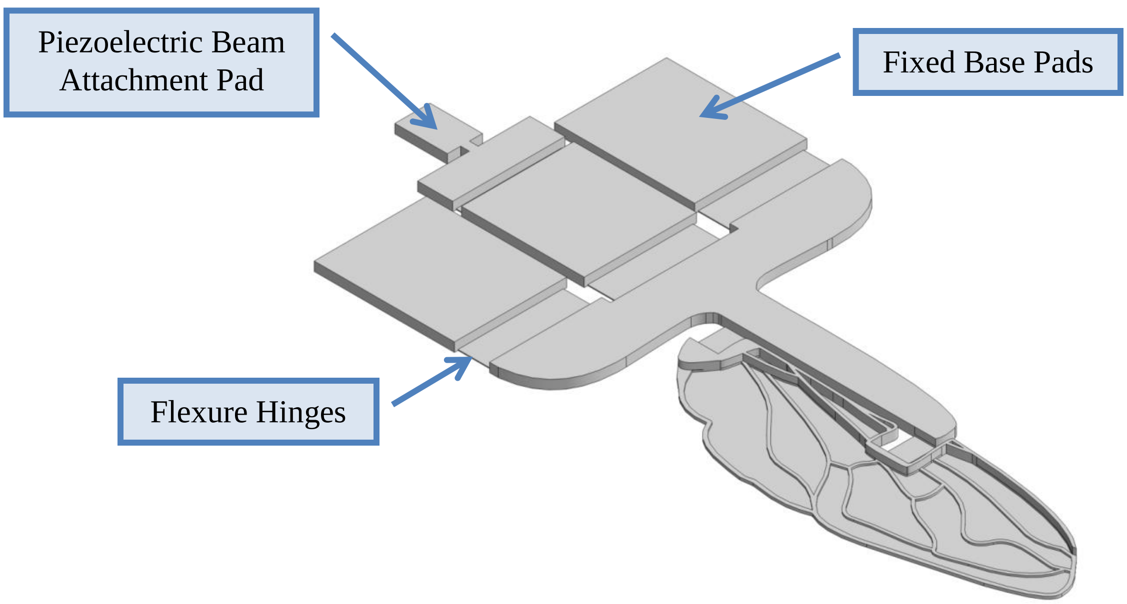

Figure 1. Eristalis Wing Geometry

Rotational motion of the nature-inspired wing is allowed entirely through the deformation of complaint flexure hinges. Compliant flexure hinges are a subcategory of complaint mechanisms, which "gain at least some of their mobility from the deflection of flexible memebers rather than from movable joints only" according to Howell [2]. In addition to a complaint mechanism, the Eristalis wing can be classified as a Microelectromechanical System (MEMS) [2]. The wing has dimensions on the micrometer scale, is manufactured in planar form from a single material, requires minimal assembly, and combines a piezoelectric bimorph with a mechanical body to achieve motion.

Eristalis Wing Operation

Before a meaningful analysis of the stresses in the Eristalis wing can be accomplished, an understanding of the set up and operating conditions of the entire mechanism are required. First, the desired geometry is etched by a photoresist process. The entire wing structure is made from "SUEX dry film, an epoxy based negative photresist" [1]. The properties of the SUEX material can be found on the website of the manufacturer DJ DevCorp [3] and are summarized in Table 1. The SUEX Material was specifically chosen for both material properties to allow large deformation and optical properties to allow for a custom construction process [1]. After the wing has been created, it is then glued by its two base pads to a rigid mount. At this point the entire sturcture is still in its planar configuration.

Table 1. SUEX Material Properties [1]

Property	Value
Modulus of Elasticity	2.8 GPa
Poisons Ratio	0.39
Yield Stress	86 MPa
Density	1190 kg/m^3
Yield Strain	3.07 %
Material Type	Linear Isotropic Elastic

Next, the tip of the piezoelectric bimorph beam is glued onto the attachment pad of the Eristalis mechanism. Now the structure is ready to be deformed to its operating position. The piezoelectric beam is then lifted vertically 0.952 mm, and then pulled horizontally until the wing reaches an angle of 77°. Both of these geometric requirements were determed by Dr. Mateti from numerous dynamic system models of the Eristalis wing hinge [1]. The base of the bimorph is then clamped in place. Now, the wing is in position and any horizontal motion of the piezoelectric bimorph tip will result in angular displacement of the wing.

The flapping wing mechanism is actuated by a piezoelectric bimorph. The tip of the piezoelectric bimorph vibrates horizontally under the application of an alternating potential difference. The horizontal displacement of the piezoelectirc bimorph tip is then transfered into wing rotation by a series of compliant flexure hinges. This is illustrated in the schematic operating diagram in Figure 2. The actual thrust production by the flapping of micro-scale wings has been considered in [1] and [4], but is not within the scope of this analysis. However, flexure hinges are also used in connecting the thin wing membrane to the rigid wing spar.

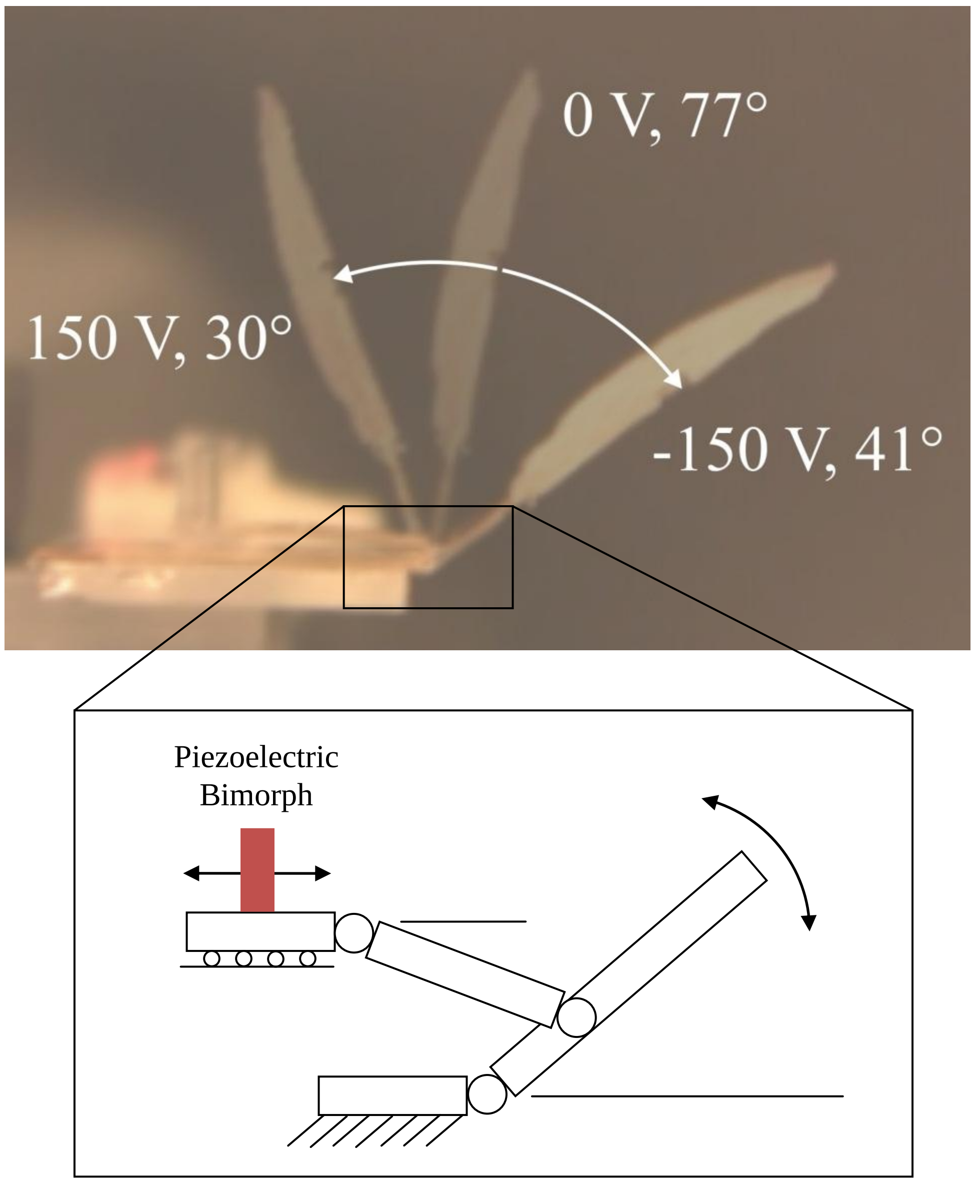

Figure 2. Eristalis Wing Operation

Photo Courtesy Dr. Mateti

The Appendix contains high definition images from Dr. Mateti that better illustrate the actual operation of the flexure hinges. In these images it is clear that the thinnest regions undergo very large deformations, while other parts are made to be rigid. The Eristalis wing flapping mechanism was designed to channel the largest deformation required about a single rotation axis. This axis is maintained by two flexure hinges, each 3 mm wide, 1 mm long, and between 15 and 25 μm thick. In comparison, the rigid body parts of the wing are over 250 μm thick.

As Smith states in [5], “Most flexure systems may be divided into two broad categories, notch and leaf type hinges.” The Eristalis wing has essentially a hybrid between a notch and leaf type hinge. The Eristalis mechanism combines the precision of a notch hinge with the large deformation potential of a leaf hinge. Examples of notch flexure hinges providing precise rotation can be seen in both microgripping applications [6] and micro-motion stages [7]. Notch flexure hinges create very well-defined axes of rotation by concentrating stresses and strains in the thinnest portion of flexures [5]. However, “as a direct consequence of this, high local stresses limit the deflection of the notch hinge. The leaf type hinge distributes the deflection over the length of the hinge, thus lowering stresses and allowing greater deflection for a given hinge length.” [5]

Simulation Goals

The goal of this thesis is to use both stress analysis theories and Finite Element Analysis (FEA) software in order to:

1. Validate theoretical models developed by Dr. Mateti.
2. Begin to explain the operational limits and structural failure of the Eristalis wing. Comparisons will be made with pictures and other data as available.
3. Understand the stresses induced in the flexure hinges. This includes not only an understanding of the bending stresses, but also the stress concentrations at sharp corners and the effect of fillets in reducing the stresses. Static as well as dynamic stresses will be considered.
4. Provide advice for future flapping-wing, nano air vehicle, compliant mechanism design based on the detailed results for the Eristalis wing.

Theoretical Analysis

The operation of the Eristalis flapping wing depends on the large deformation of complaint beams. As illustrated in Figure 2, the wing hinges cycle between displacements of 107° and 41°, angles well above the small curvatures at which the assumptions of the Bernoulli-Euler beam equations for small deformations are valid. Figure 3 displays an example of the highly nonlinear beam bending for the SUEX material. In the wing operation, the flexure hinges are given a defined displacement as governed by the enforced motion of the piezoelectric bimorph tip. Therefore, the following beam models will start with a prescribed beam tip angle, theta, and then the equations will be used to solve for the force required to produce such an angle. This force will be used to solve for the stress in the flexure hinge.

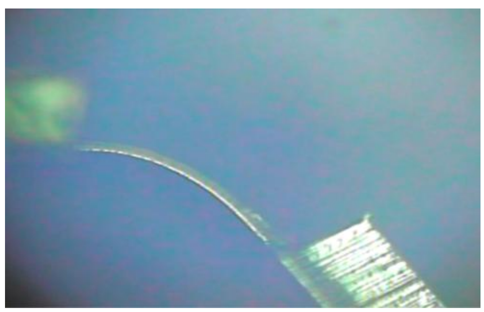

Figure 3. Eristalis Flexure Hinge Bending
Photo Courtesy Dr. Mateti

The difference between applying a displacement load and a force load is also explained by Howell in *Compliant Mechanisms* [2]. For force loads, stress is decreased by increasing the stiffness. But for displacement loads, “the stress is decreased by decreasing the stiffness” [2]. And, decreasing the stiffness of a beam can be “accomplished by using a material with a lower Young’s modulus, or by decreasing the moment of inertia” [2]. Both of these measures have been undertaken by Dr. Mateti to make the Eristalis wing hinges as robust as possible. Still, failures of the wing hinges during operation warrant the further exploration of the Eristalis wing’s specific geometry and operating conditions in the following theoretical models.

Large Deformation Beam Equations

The beams in the flexure hinge are specifically designed to undergo large deflections. According to Dr. Mateti, "the flexure lengths are designed to bend at a maximum of 60º and the flexure widths are designed to prevent buckling." [1]

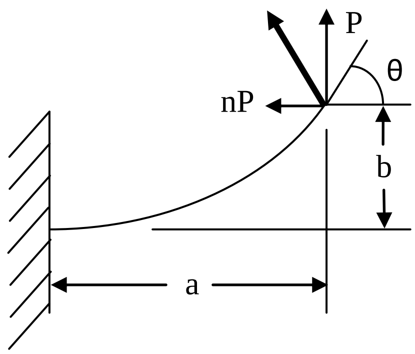

Figure 4. Large Deformation Beam

The procedure and derivation of the beam equations is covered in [2] for a Cantilever Beam with a force at the free end (pg 47, section 2.9.2).

$$\lambda = \sin\theta_0 - n\cos\theta_0$$

$$\alpha = \frac{1}{\sqrt{2}}\int_0^{\theta_0}\frac{d\theta}{\sqrt{\lambda - \sin\theta + n\cos\theta}}$$

$$P = \frac{EI\alpha^2}{l^2}$$

In order to find the beam tip trajectory and calculate the moment arms for the bending moments, values a and b must also be calculated.

$$b = \frac{l\sqrt{2}}{2\alpha}\int_0^{\theta_0}\frac{\sin\theta\, d\theta}{\sqrt{\lambda - \sin\theta + n\cos\theta}}$$

$$a = \frac{l\sqrt{2}}{2\alpha}\int_0^{\theta_0}\frac{\cos\theta\, d\theta}{\sqrt{\lambda - \sin\theta + n\cos\theta}}$$

The bending stress is given by:

$$\sigma = \frac{Mc}{I} = \frac{Mt}{2I} = \frac{(Pa + nPb)t}{2I}$$

The numerical capabilities of Matlab can be used to solve the elliptical integrals required to find the force required to produce the predetermined beam tip angle [8].

Pseudo-Rigid-Body Model

A structure can be simplified for analysis by replacing flexure hinge components with representative rigid body elements. In this case, the flexure hinges will be replaced with torsional springs. The equations that follow are derived for a beam with a force at its free end, from the procedure as outlined by Howell for a beam with a moment at the end [2]. The maximum angle theta for a cantilever beam with a force at the free end is [2]:

$$\theta_{max} = \frac{Fl^2}{2EI}$$

The equation for a torsional spring is given by $T = K\theta_{max}$, where *T* is equal to Fl.

Therefore, the torsional spring constant, *K*, can be found:

$$K = \frac{2EI}{l}$$

The bending stress is given by:

$$\sigma_{max} = \frac{Mc}{I} = \frac{Tt}{2I} = \frac{(K\theta_{max})t}{2I}$$

Substituting for K:

$$\sigma_{max} = \frac{\left(\frac{2EI\theta_{max}}{l}\right)t}{2I} = \frac{Et\theta_{max}}{l}$$

Buckling

The axial component of the flexure hinge loading creates the possibility of a buckling mode. Complaint beams can be purposely designed to buckle and form a certain desired shape [9]. Because the beam in the Eristalis flexure hinge is lifted vertically before an axial stress is applied, the possibility of bucking is minimized. Nonetheless, the critical buckling load will be calculated for the flexure hinge at low angles of theta. As presented in [9], the critical buckling load is defined as [10]: $P_{cr} = \frac{\pi^2 EI}{\left(L_{eff}\right)^2}$

Matlab Code

Matlab has been utilized to both calculate and visualize the results of the theoretical models. Figure 5 shows the variation in bending stress for flexure hinge geometry using the large displacement model.

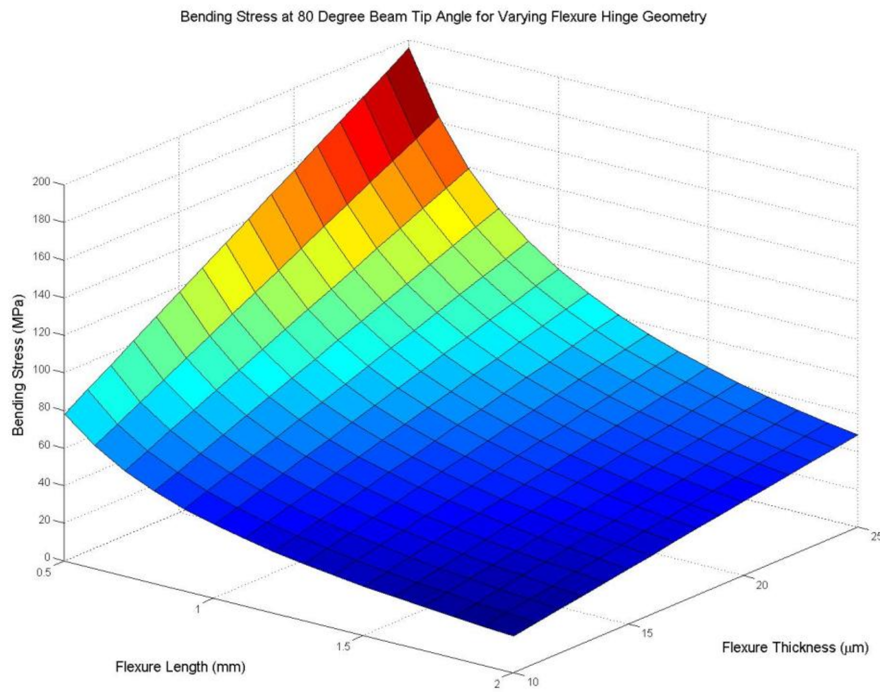

Figure 5. Matlab Surface Plot

This plot can be used to help design a flexure hinge that is required to undergo large deformations. A combination of length and thickness that allow for an appropriate precision of rotation while maintaining allowable stress levels is desired. The plot has been given axes that capture the actual length used in the Eristalis wing (1mm length, 15-25 um thickness) as well as the lower limits possible for thickness given current manufacturing techniques.

Another valuable output from Matlab is a plot of bending stress vs. beam tip angle for angles from 0 to 120 degrees. Ansys stress results have also been read into Matlab for comparison to the theoretical models. These plots will be presented after the development and use of the Ansys 2D Beam Model is discussed.

Finite Element Analysis Overview

A goal in analyzing the Eristalis wing will be to utilize a Finite Element Analysis (FEA) program to gain a complete understanding of stresses, resultant geometry, and wing flapping performance capabilities. The general approach will be to start with the simplest possible model of the wing hinge mechanism, and progress to a more complex and complete model. As will be seen, the high aspect ratio of the flexure hinges (3mm x 1 mm x 15 µm) drives the need for an extremely large number of elements to create a proper model using 3D elements. This increases the complexity of the model and demands a much longer preprocessor and solution time. For these and other reasons, working first with a simple model is an important step in a Finite Element Analysis process. For example, a micro-positioning system can be modeled accurately with both beam elements and 2D solid meshed elements [11]. This approach will be adapted to the Eristalis wing hinge. First, a beam element model will be created, followed by a 3D tetrahedron element model, and finally a 3D hexahedron element model. The increasing complexity of each model will be noted, and the results of each model will be compared.

Limitations and Advantages of Finite Element Analysis Software

There are numerous commercially available FEA software packages in use today. All have their relative strengths and weaknesses. But a common theme remains: high performance computers have made it possible to solve very large Finite Element models in short periods of time. However, a FEA software package is only as capable as its operator.

SolidWorks and Ansys will be used to conduct a comprehensive analysis of the stresses in the Eristalis wing mechanism. SolidWorks is not exactly a FEA program, but it has a much better user interface for Computer Aided Design (CAD) than Ansys. Therefore, SolidWorks was used to prepare the Eristalis geometry for analysis in Ansys. SolidWorks does have a modest FEA plug-in program, but users are limited to tetrahedron elements. On the other hand, Ansys is a very powerful FEA program. Ansys offers users much more control over the element types, loading, solver parameters, and post processing of results.

Nonlinear Analysis

The Eristalis wing geometry experiences a geometric nonlinearity [12]. This means that the stiffness of the wing hinge structure changes dramatically as it is deformed from a planar position into a proper angled position. This process is completed by epoxying the tip of the piezoelectric beam actuator onto the attachment pad of the wing mechanism and then lifting the tab first vertically, and then horizontally to produce an initial angular displacement of the wing. Only after these first two steps can the wing begin to flap. The large and unique nature of the nonlinearity in the Eristalis wing model demands extra care in setting up a finite element model.

Ansys Beam Element Model

It is often advantageous to represent 3D geometries using 2D elements in FEA programs [12, 13]. In the case of the Eristalis flexure hinges, the finite element model can be greatly simplified by using 2D beam elements instead of 3D tetrahedral or hexahedral elements by making an assumption about the wing operation. The beam model will only allow for a pure bending stress condition. In the development of finite element equations, a beam element is classified as being a "long, slender structural member generally subjected to transverse loading that produces significant bending effects as opposed to twisting or axial effects" [13]. The Eristalis wing does not fit this description perfectly, but bending is clearly the dominant deformation mode. By making this beam assumption, the model is reduced to less than 50 elements using 2D beam elements, whereas tens of thousands of elements will be used to create a finely meshed 3D model.

In order to define a beam element, two end nodes, material properties, and a cross-sectional area profile are required. While the results with beam elements will be limited compared to the 3D model, the solution time is drastically lower. Using BEAM189 elements in Ansys will not allow detailed stress outputs, but will give the curvature of the beam, reaction forces, and the principle bending stress at each node [12].

The validity of the pure beam assumption will be assesed after running both 2D and 3D models. The Transient Analysis solver in Ansys allows a model with time dependent loads to be solved. For the purposes of the Eristalis wing, the Transient Analysis solver will be used in two different ways, a Static Analysis and a Dynamic Analysis.

Model Creation

The Ansys beam element model is created by first defining Keypoints at the edges of each beam section. Next, lines are created between Keypoints. Then, Beam Sections must be defined. Ansys supports several types of beam cross section profiles, but the Eristalis wing requires only rectangular cross sections. Table 2 displays the information required to define the four beam sections found in the Eristalis model.

Table 2. Beam Sections

Beam Section Number	Name	Width (mm)	Thickness (um)
1	Outer Flexure	6	15-25
2	Inner Flexure	3	15-25
3	Outer Body	6	260
4	Inner Body	3	260

After defining the Beam Sections, each line must be meshed. Lines are meshed by specifying the element type, element size, material, and beam section. The lines must be meshed while they are still in planar position. However, after applying the load steps for displacement it is easier to visualize the relationship between the lines and elements in the model. Figure 6 shows the Eristalis wing, where each beam link is modeled with only one beam element.

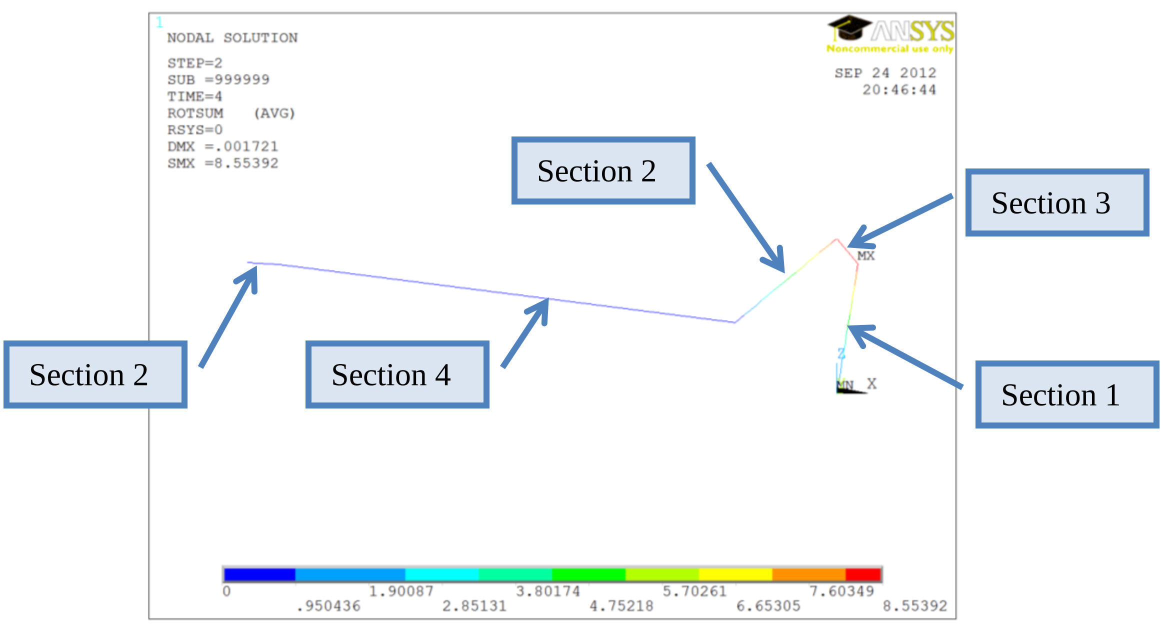

Figure 6. Ansys Beam Model, 1 Element Flexures

While at first the elements still just look like lines, after issuing a command to display the beam section representation (/ESHAPE, 1), Ansys displays the full beam section profiles [14] as can be seen in Figures 7 and 8. Additionally, once a working model has been established, the mesh must be refined to generate more accurate results. Instead of only one element representing each beam section, multiple beam elements can be used. Figures 6-8 illustrate the smoothing effect the element refinement has on the deformation of the flexure hinges.

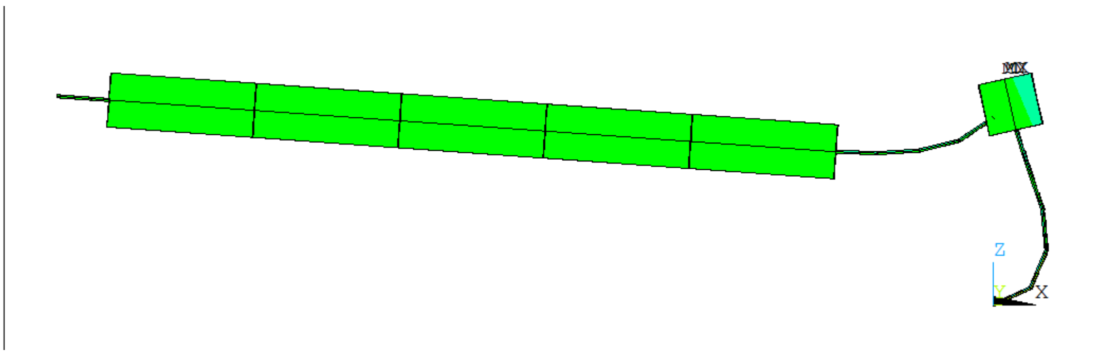

Figure 7. Side View, 5 Element Flexures

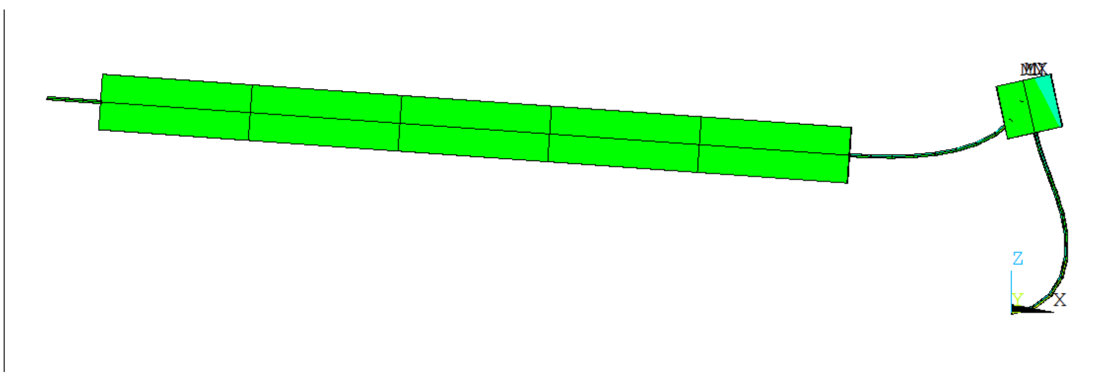

Figure 8. Side View, 10 Element Flexures

The addition of elements to model the flexure hinges can also be observed to check for a convergence of the finite element solution towards an “exact solution” [13]. This is done by plotting a characteristic stress result versus the number of elements used to model the geometry. This technique is applied for the maximum bending stress in the flexure hinges in Figure 9. The beam model with 20 elements per flexure hinge produced the same maximum bending stress at 1 mm of horizontal displacement as the beam model with 10 elements. The plot shows that mesh refinement can stop at 10 elements for each of the large deformation flexure hinges because the difference in results becomes negligible relative to the extra time required for a solution with more elements.

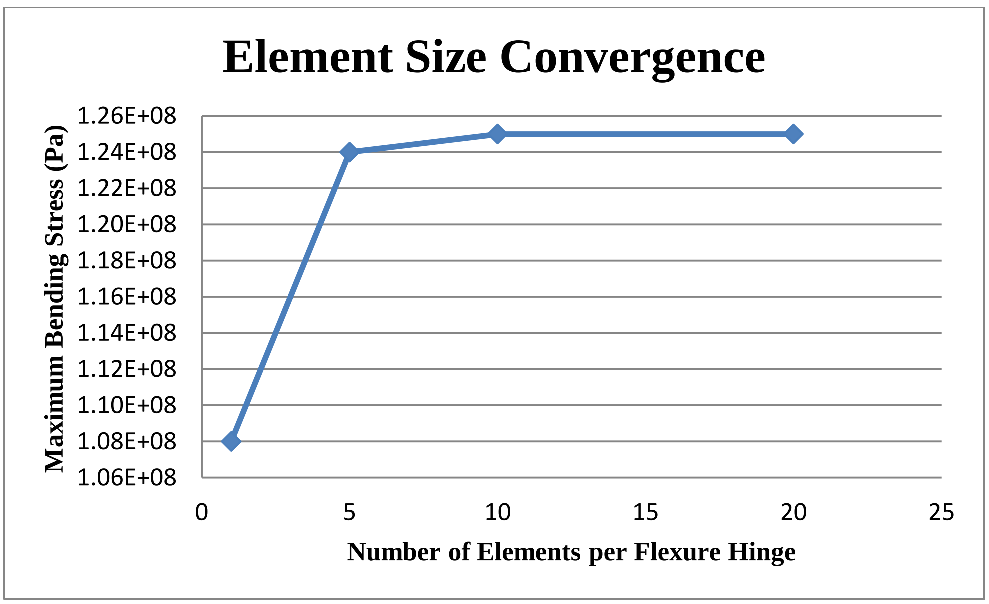

Figure 9. Element Size Convergence Plot

Static Analysis

Time will be used as a non-dimensional parameter in the Transient Analysis to define custom load steps for the wing hinge and represent a “static” analysis. For example, time steps are on the order of multiple seconds for this solution. The first load step to lift the piezoelectric attachment 1 mm vertically will be applied over five seconds. Similarly, the second load step will move the piezoelectric attachment 1 mm horizontally over ten seconds. Within each load step, substeps are used to apply the defined load over smaller ramped increments. A larger time period and more substeps are prescribed for the second load step, as this is where the deformation will be the largest. Table 3 provides a summary of the different load steps. Even though time here is considered non-dimensional, applying a static displacement over a longer time period is actually representative of how Dr. Mateti initially tested static displacement. Voltage across the piezoelectric bimorph was slowly ramped upwards and downward over multiple seconds. The static response of the Eristalis wing can be seen in the Appendix.

Table 3. Static Analysis Load Steps

Load Step	End Time (Seconds)	Substeps	Load
1	5	20	UZ = 1.0 mm
2	15	100	UX = -1.0 mm

For the static analysis, the wing spar is left out of the model. But, a vertical force must be applied to the remaining wing body in order to give a pre-curvature to the flexure hinges before the horizontal motion of the piezoelectric pad. The horizontal motion required to bring the wing to its initial angle is meant to ‘pop’ the wing into its proper curved position. After running several models, it was observed that if the beam is not initially curved before the horizontal displacement begins, there is a strong tendency for the beams to simply buckle instead of bend. Figures 10 and 11 illustrate the bending stress in the deformed Eristalis mechanism for different levels of element mesh refinement.

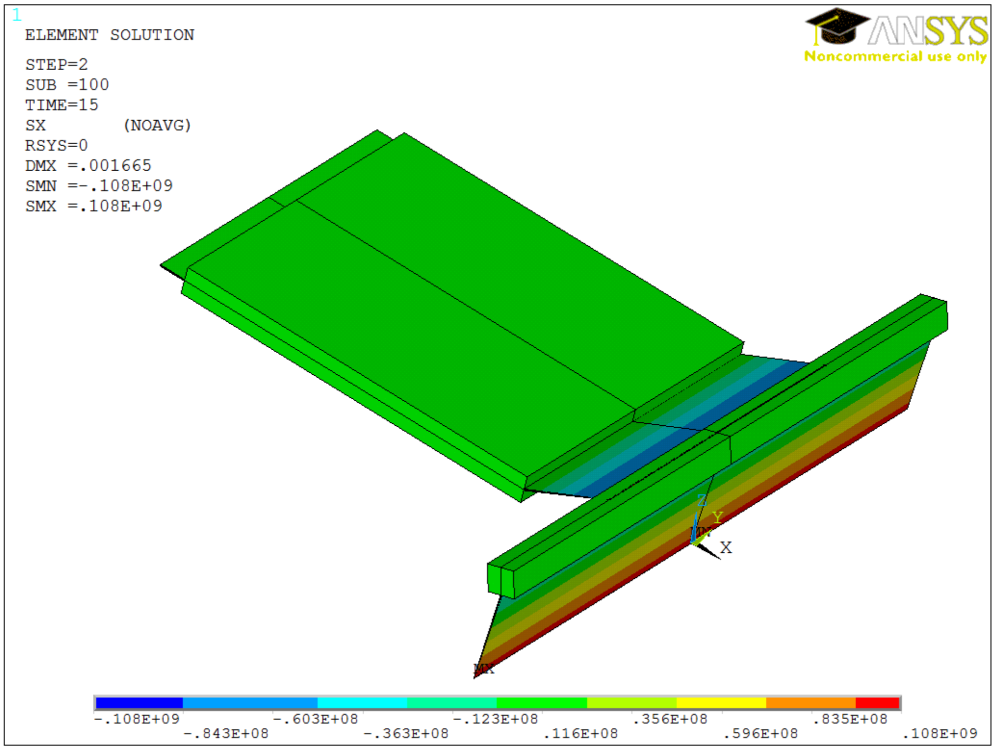

Figure 10. Bending Stress Contour Plot, 1 Element Flexures

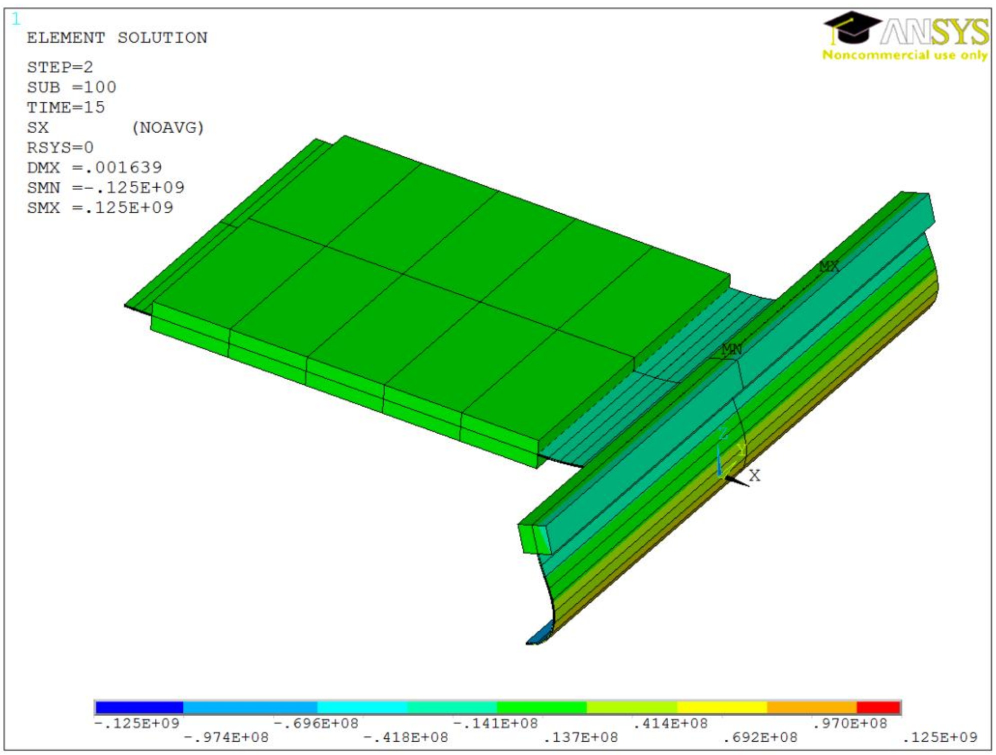

Figure 11. Bending Stress Contour Plot, 10 Element Flexures

Compared to Figure 10, the static beam deformations seen in Figure 11 are more representative of the actual beam deformations as seen in the Appendix. This reinforces the earlier conclusion that representing the flexure hinges with ten elements is appropriate.

Results in Ansys can also be exported to data files instead of simply visualized in the Ansys window. The maximum bending stress and wing angle are recorded for each load substep in the solver. The flexure thickness of the mechanism is varied between the current limits of the construction process, and the results are plotted using Excel. It can be seen that at higher angles the bending stress surpasses the yield stress of the SUEX material, 86 MPa.

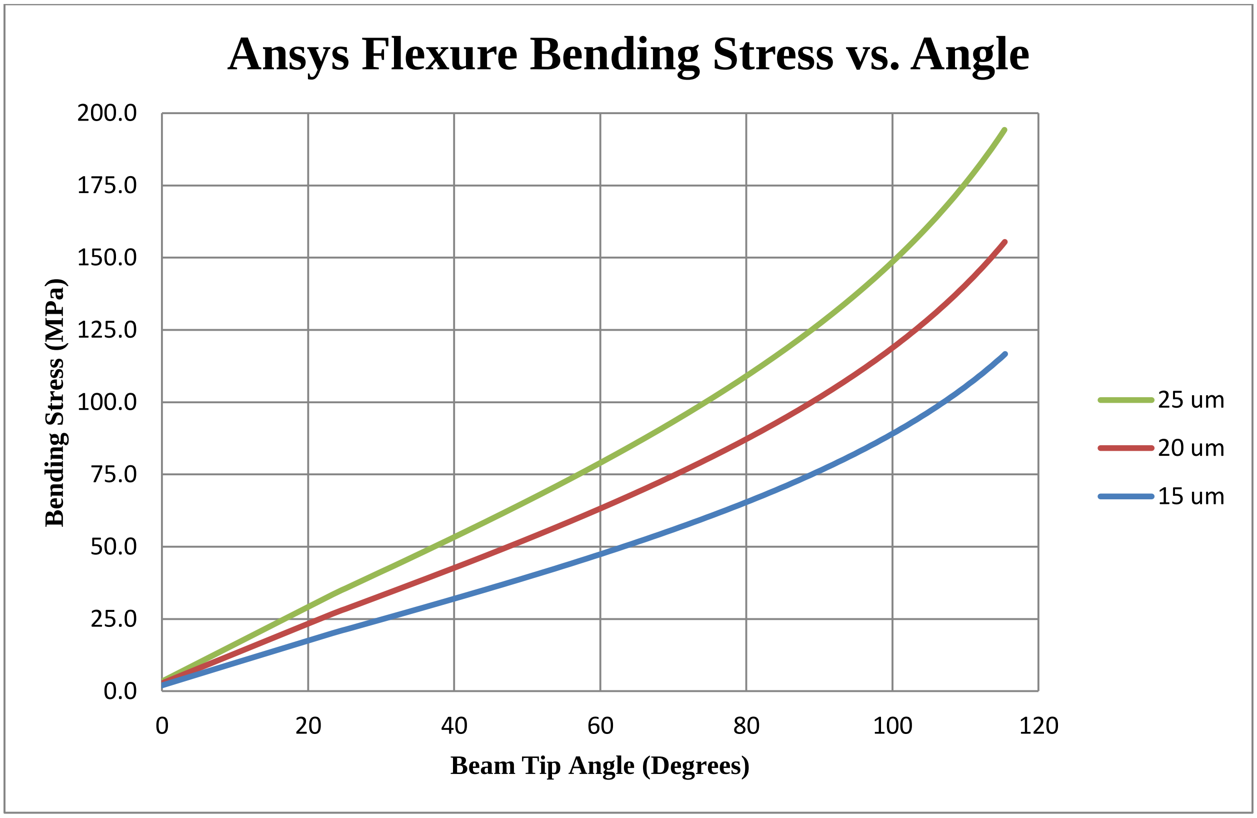

Figure 12. Ansys Flexure Bending Stress vs. Angle

The results in Figure 12 can also be imported to Matlab and plotted with the results of the theoretical stress calculations for flexure hinge bending. Figures 13 and 14 show a comparison between bending stress and reaction force among models.

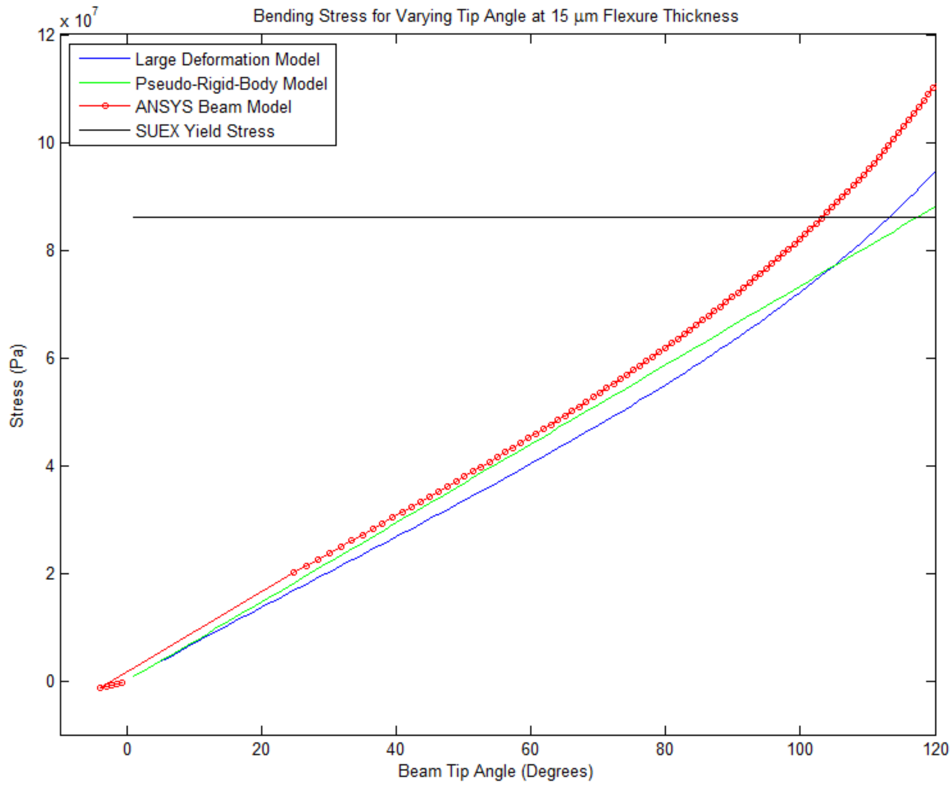

Figure 13. Bending Stress for Varying Beam Tip Angle

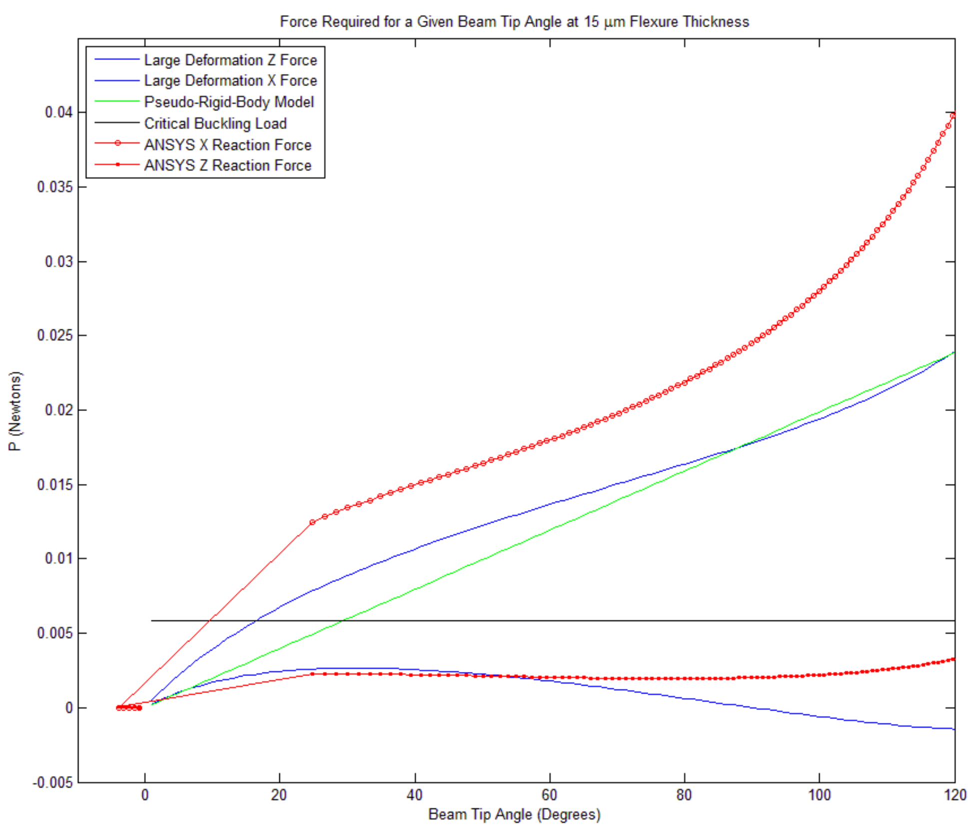

Figure 14. Reaction Force for Varying Beam Tip Angle

Ansys can also animate results over time for a transient analysis. Frames in Figure 15 can help explain the response of the Eristalis wing to the two different load steps. Notice between frames 2 and 3 how the wing body suddenly pops into the proper bending mode.

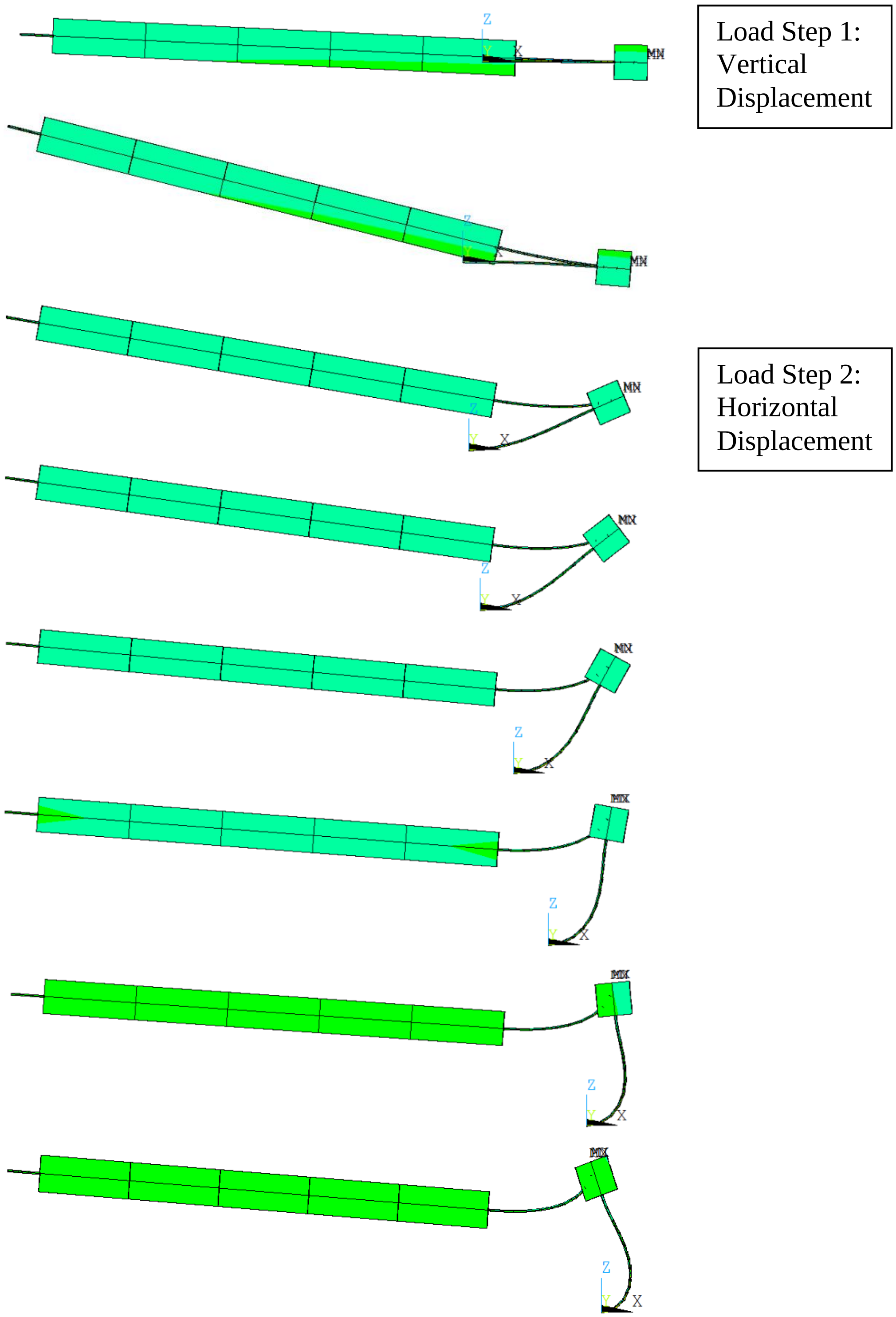

Figure 15. Static Response Animation

Dynamic Analysis

Once the static model is running properly, time will be used as an actual parameter and displacement loads will be applied at the actual operating frequency used in flapping the Eristalis wing. For example, in experimental operation 150 Volts are applied across the piezoelectric bimorph at a frequency of 50 Hz, determined to be the natural frequency of the Eristalis wing [1]. To represent this, a sinusoidally varying force load will be applied to the piezoelectric attachment pad. Also, as can be seen in Figure 16, a wing spar needs to be added to the dynamic model, as the mass properties are now significant.

To run the analysis, the first two load steps from the static analysis remain the same. But now a third load step is defined, the sinusoidally varying force load. The load is applied as a ramped sinusoid, and the magnitude of the maximum force is given by the blocking force of the piezoelectric bimorph. The blocking force for typical piezoelectric beams used in the Eristalis mechanism is approximately 40 mN [1]. Since it is not possible to run a modal analysis on the displaced structure, it will be difficult to find the natural frequency of the Eristalis mechanism for operation.

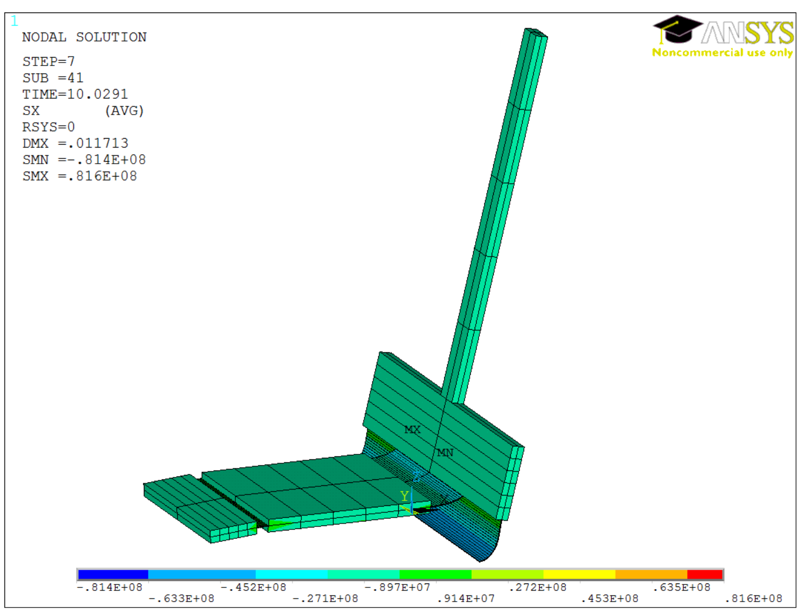

Figure 16. Eristalis Wing for Dynamic Analysis

Applying the blocking force to the piezoelectric attachment pad at 50 Hz did not cause any significant displacement after multiple trial runs. Instead, to try and see more amplification of the wing rotation, a +/- 0.1 mm displacement load was applied at 47 Hz to the attachment pad. This displacement range is roughly the maximum tip displacement capable of being produced by the piezoelectric used in the Eristalis wing mechanism [1].

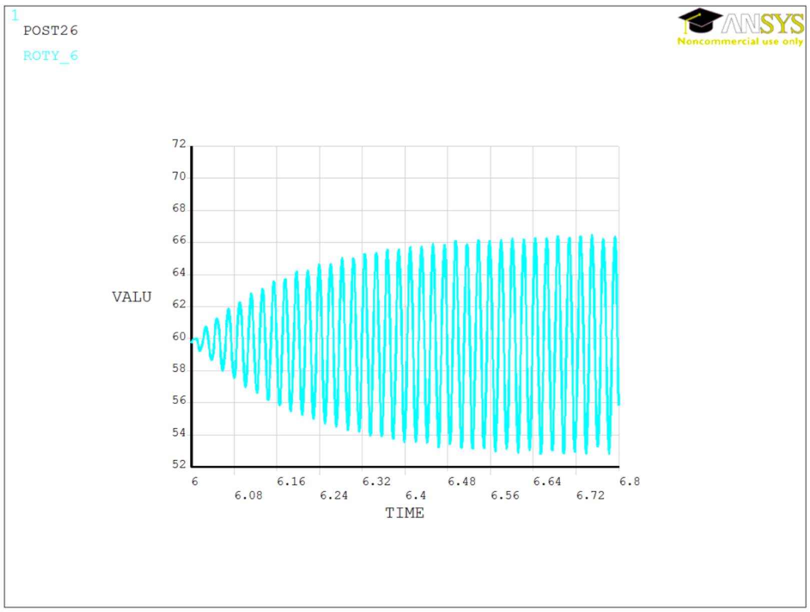

Figure 17. Wing Spar Rotation

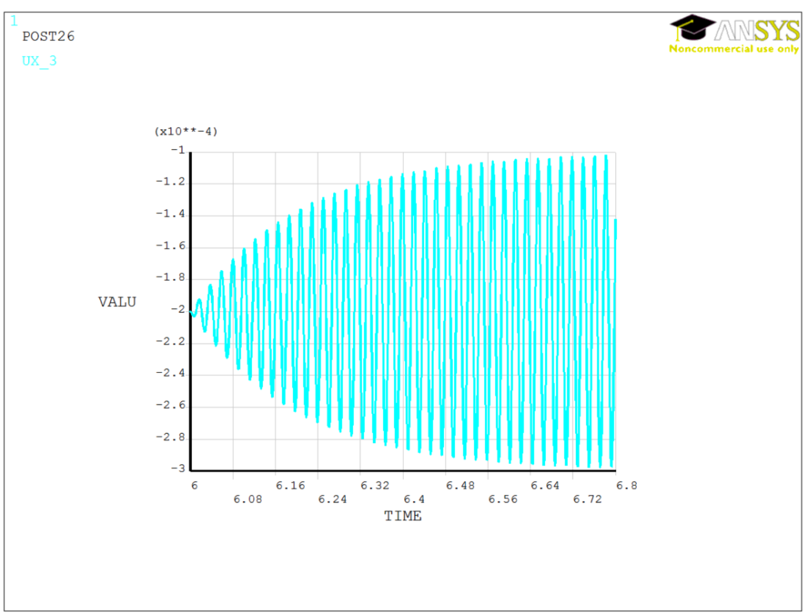

Figure 18. Piezoelectric Attachment Pad Horizontal Displacement

Results

The collection of results from the Ansys beam models show a strong similarity to the stress values predicted by the two theoretical models. The theoretical and Ansys models indicate that the bending stress becomes greater than the yield stress of the SUEX material at beam tip angles above 100º, as seen in Figure 13 for a 15 µm flexure thickness. The stress is even higher for thicker flexures. The Ansys model gives the smallest angle to reach the yield stress at 104º, which is within the operating angle range as seen in Figure 2. The behavior of the SUEX material is not known past the yield stress of 86 MPa. Regardless, it is desirable to operate the wing below its yield strength.

A method for simulating the actual operation of the flapping wing has been developed. After applying the initial displacement to the hinges, a load can be applied as a sine function at a desired frequency. The small flap angle of 14º shown in Figure 17 may mean that the resonance frequency of the Ansys model is different than the experimentally determined frequency of 50 Hz.

SolidWorks Model

The SolidWorks Simulation plug-in for SolidWorks 2012 will be used as an intermediate step in the 3D Finite Element Analysis process. SolidWorks will be used to prepare the solid model geometry before transfer to Ansys.

Geometry Preparation

The process began with the Eristalis wing SolidWorks model provided by Dr. Mateti. The design, construction, and testing of this device is again described in great detail in [1].

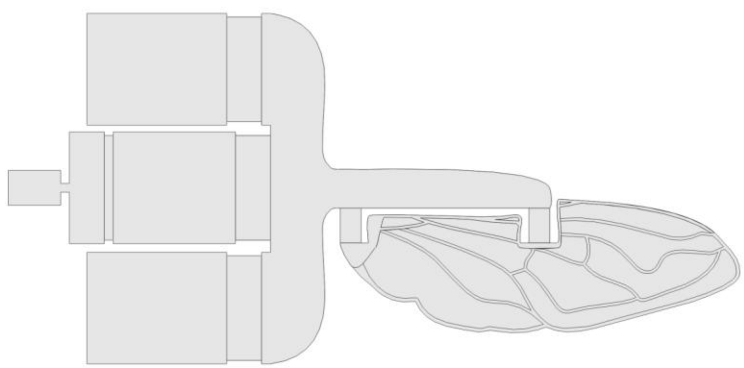

Figure 19. Flat Eristalis Wing and Hinge Mechanism Top View

Symmetry was added about the central plane of the wing mechanism in order to reduce the number of mesh elements required.

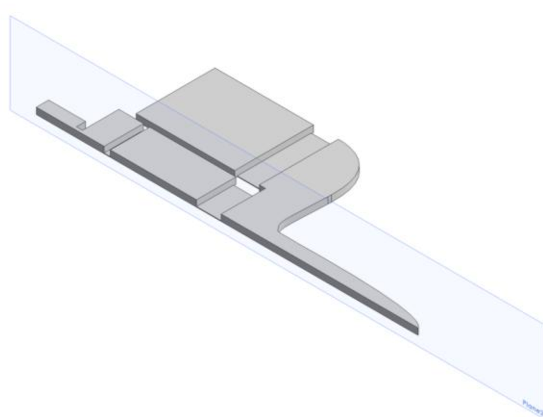

Figure 20. Eristalis Wing Plane of Symmetry

Next, the wing itself is removed. When analyzing the wing hinge at a static displacement, the wing does not affect the hinge position and stresses. The rotational inertia of the wing is very important for dynamic analysis, but in the static analysis the stresses in the hinge due to the piezoelectric attachment pad displacement are much larger than the contribution from gravity on the wing. Therefore, the wing is also removed to lower the number of mesh elements and allow for faster computing.

Sharp corners from the original SolidWorks model are chamfer filleted in Figure 21. Filleting the edges of the sharp corners prevents the model from analyzing large stress concentrations which can cause singularities during the analysis. Not only do the fillets help with the simulation, but adding the fillets actually is a better physical representation of the flexure hinges as a result of the manufacturing process. While the SolidWorks model originally included sharp corners at all edges, the realities of the photo resist manufacturing process creates fillets at the edges of all flexure hinges as seen in Figure 22. The radii of these fillets are approximately 30 µm.

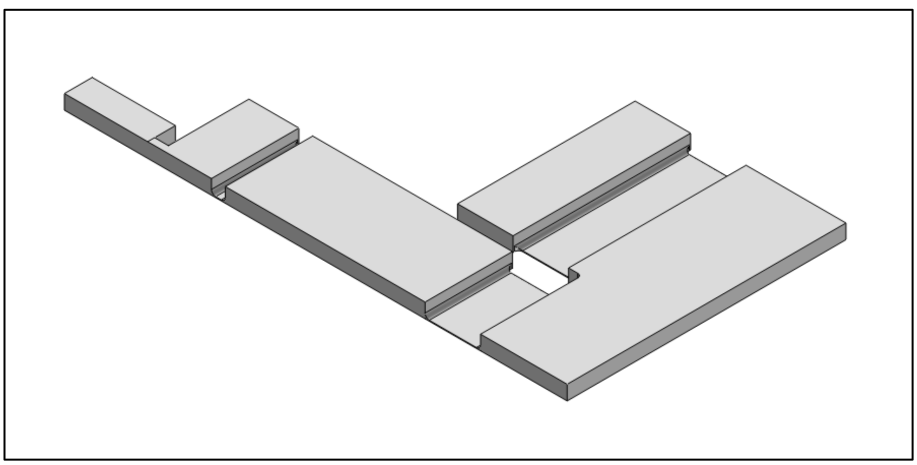

Figure 21. Simplified Eristalis model for stress analysis

Now that the geometry of the wing has been altered, the material properties must be specified for the Finite Element Analysis. SUEX material properties are listed in Table 2.

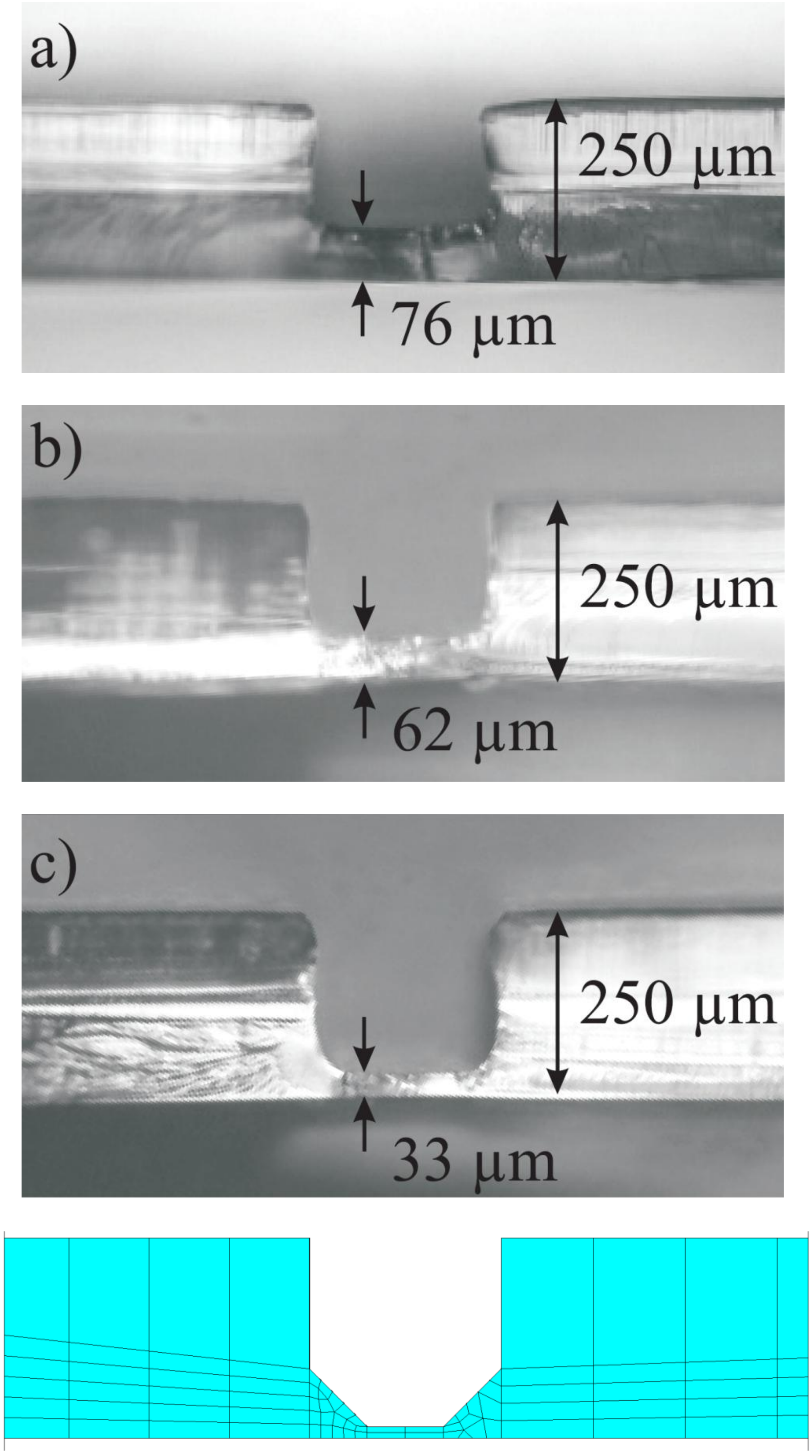

Figure 22. Actual vs. Finite Element Flexure Hinge Fillets

Photos Courtesy Dr. Mateti

Meshing

SolidWorks 2012 only has tetrahedral element meshing capabilities [15]. Geometries are most easily meshed with tetrahedrons, as they can be combined to form almost any shape with minimal user input. In SolidWorks, all the user has to specify is a mesh density ranging from coarse to fine, and then click “mesh”. Mesh refinement can still be done along curves or surfaces as seen in Figure 23, but SolidWorks allows nowhere near the customization that Ansys does.

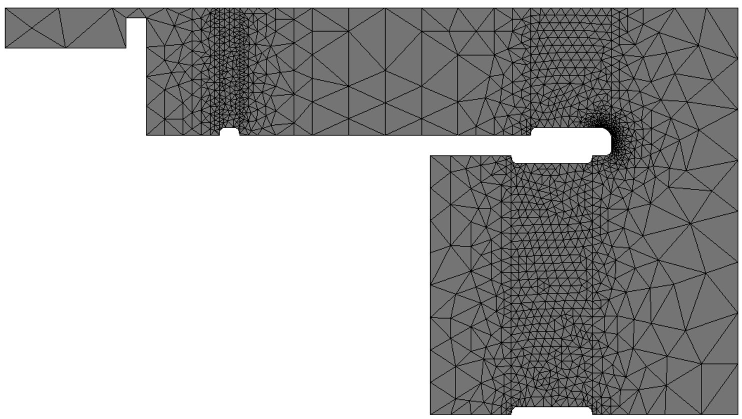

Figure 23. SolidWorks Mesh with Refinement on Flexures and Corners

The problem is exaggerated in the Eristalis model as it is prone to high stress concentrations due to sharp corners, large displacements, and large stresses. When multiple models were run in SolidWorks, almost all of the models failed before reaching their full prescribed horizontal displacements due to stress concentrations and bad element configurations. This can be partially attributed to the poor mesh quality generated by SolidWorks. It is impossible to view all of the elements inside the structure using SolidWorks, so even though all of the elements may look good on the surface, the aspect ratios of elements inside the model may be poor. For example, the model showcased in Figure 23 has the following mesh properties taken from Figure 24. The mesh quality is described as “High”. However, 0.118% of elements have aspect ratios greater than 10. With 12703 elements, this means that 15 elements could be causing very poor results and stress singularities which will terminate an analysis. An ideal analysis would have more elements with lower aspect ratios. However, the complex geometry of the Eristalis mechanism makes it difficult for the automatic generation of a quality mesh.

Mesh Details

Study name	Study 3 (-Default-)
Mesh type	Solid Mesh
Mesher Used	Curvature based mesh
Jacobian points	4 points
Mesh Control	Defined
Max Element Size	0.563555 mm
Min Element Size	0.112711 mm
Mesh quality	High
Total nodes	23141
Total elements	12703
Maximum Aspect Ratio	13.442
Percentage of elements with Aspect Ratio < 3	73.2
Percentage of elements with Aspect Ratio > 10	0.118
% of distorted elements (Jacobian)	0
Time to complete mesh(hh:mm:ss)	00:00:02
Computer name	PCSTUDIO21

Figure 24. SolidWorks Mesh Details

Several models were solved in SolidWorks, but with limited success. Therefore, the results of the SolidWorks simulations will not be presented. More importantly, the experience gained from learning about the limitations of the SolidWorks Simulation plug-in has led to the motivation for a more in-depth finite element formulation using Ansys.

Ansys 3D Element Model

The limited capabilities of the SolidWorks Stress Analysis module provide the motivation to continue the analysis of the Eristalis wing using Ansys. The ability to use custom element types, define more specific load steps, and a more robust solver will lead to increased accuracy. The goal will be to first analyze the stresses caused by the static displacement of the wing, and then comment on the results relative to the 2D Beam model.

Importing the Geometry from SolidWorks

The Eristalis model created and analyzed in SolidWorks was then saved as a STEP file and imported to Ansys Version 14.0 operating with the Ansys Academic Research license. The Academic Research license allows an unlimited number of nodes for mesh generation.

Meshing

Ansys allows the use of several different element types. It is often necessary to solve a load case using multiple variations of these element types, as no single finite element calculation alone can stand as an exact solution. Higher order element types often produce better results for large deformations, but at the cost of more computer processing time. The distinction between tetrahedral and hexahedral, or brick, elements can also be critical for FEA models. Brick elements cannot be meshed to the complex geometry of the Eristalis very easily. Whereas the tetrahedral elements can simply be created with a “free” mesh, hexahedral brick elements must either be “mapped” or “swept”. In this case, elements will be swept from surface to surface. Results will be compared for different element types in order to observe the ability of different element types to accurately model large deformations.

It is important to note that a large number of elements are required to properly model the flexure hinges because of their high aspect ratios. The hinge itself may have a high aspect ratio, but the FEA elements that are created to model the hinge must have low aspect ratios to produce accurate results [13]. It is also desirable to have multiple elements in regions that undergo large strains. Both of these requirements make the number of elements in the model rise very quickly, and dramatically increase the solver time. For example, if three elements are desired across the flexure thickness of 15 µm, and for ideal cube geometry, then modeling a single flexure hinge with solid elements would require 360,000 elements. Figure 25 does not have enough elements, but Figure 26 may have too many elements for an efficient solution. A refinement level between Figures 25 and 26 will be utilized for the Eristalis hinge.

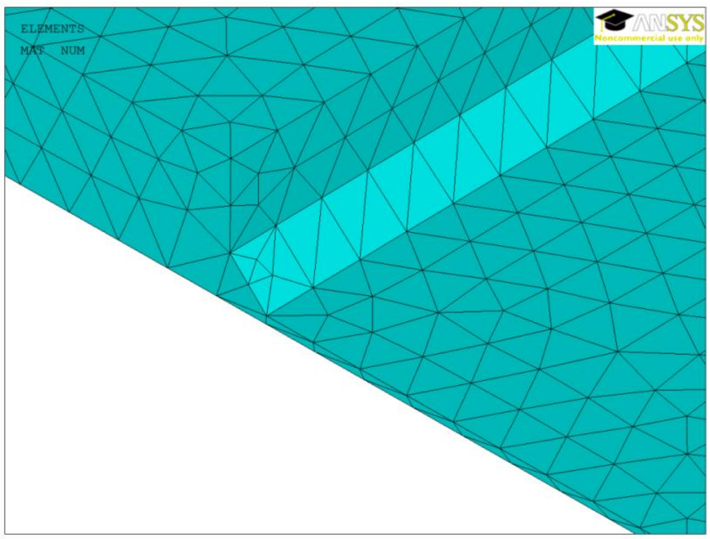

Figure 25. Example of 4 Node Tet Elements, No Refinement

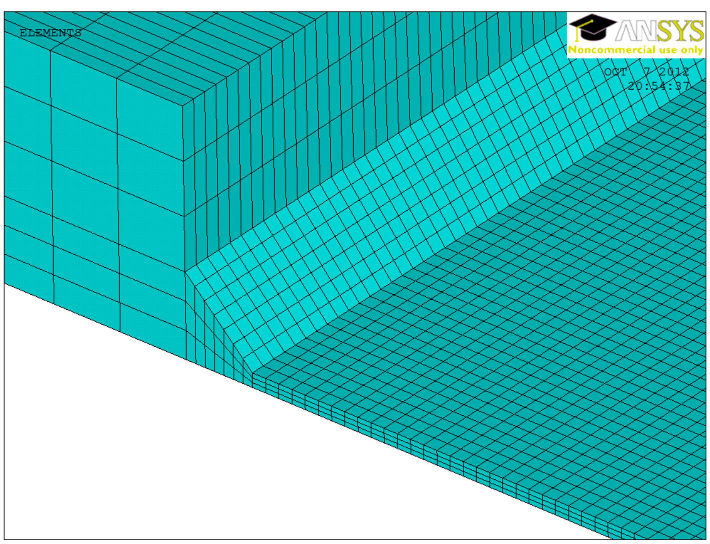

Figure 26. Example of 8 Node Brick Elements, Mesh Refinement

Applying Loads

In order to simulate the displacement path the piezoelectric attachment pad must follow, several load steps will be defined in Ansys. In Ansys, a load must be specified and then saved as a given load step. This gives a highly customized approach, for within each load step the user can assign different time stepping and solver properties. Multiple load cases can be defined, and then solved sequentially. In this case, two load steps will be defined. The first load step will consist of a 1.0 mm vertical displacement of the piezoelectric attachment pad. The second load step will consist of a -1.0 mm horizontal displacement of the piezoelectric attachment pad. These are the same loads as specified in Table 3. However, fewer substeps will be used for each load step to keep a reasonable solution time. Boundary condition loads must also be applied. The boundary conditions for the model include symmetry on the central plane of the wing and a fixed constraint on the base pad.

Results

Figures 27 and 28 show the nodal solution for von Mises stress in the Eristalis flexure hinges at a large deformation. The maximum von Mises stress in the model with tetrahedral elements is 523 MPa, while the maximum von Mises stress in the model with brick elements is 179 MPa. The value for the brick element model is much closer to the stress levels predicted by both the theoretical and 2D beam models. Figures 29 and 30 show a close up plot of the elemental solution for von Mises Stress in the Eristalis flexure hinges at a different angle. It is evident that the brick element model produces cleaner stress results due to the uniformity of the element size and better element governing equations.

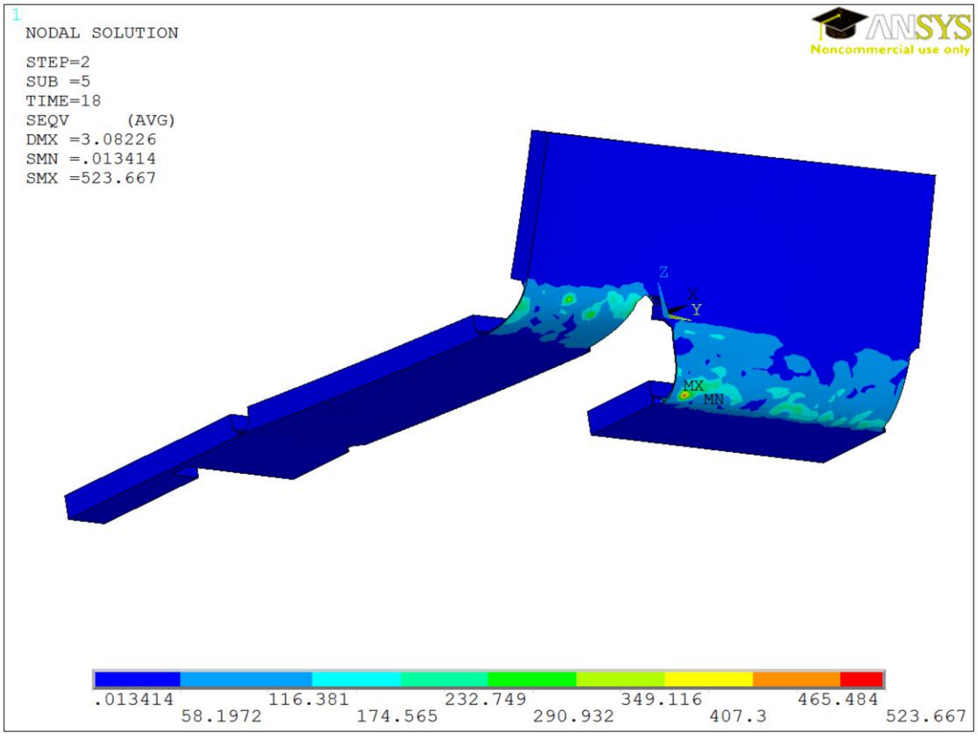

Figure 27. Von Mises Stress, 4 Node Tetrahedral Elements

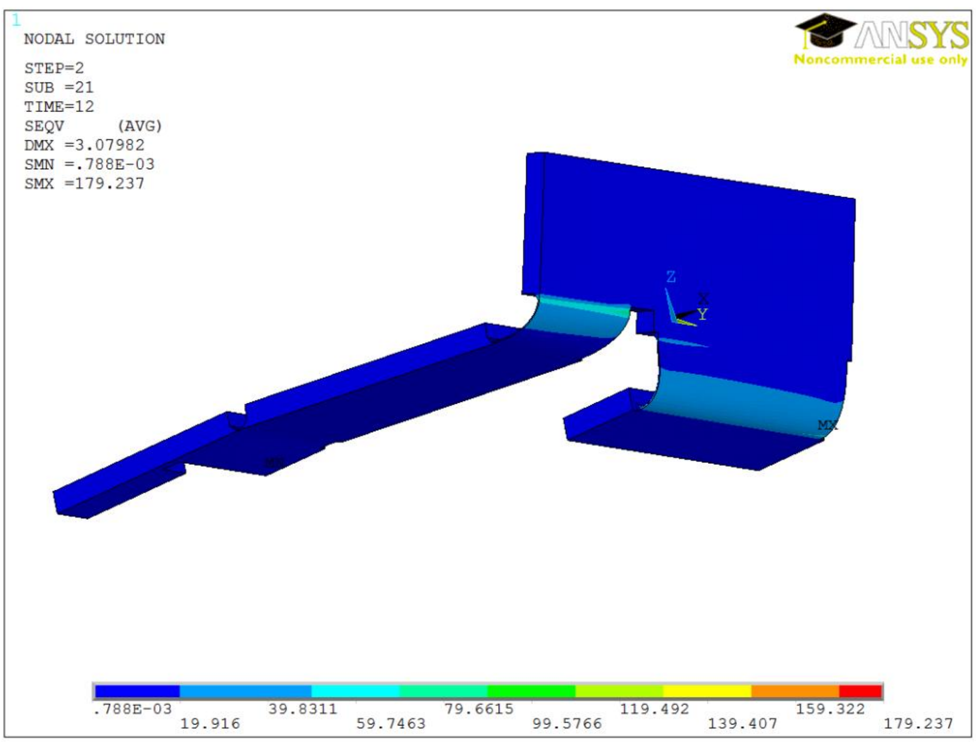

Figure 28.Von Mises Stress, 8 Node Hexahedral Elements

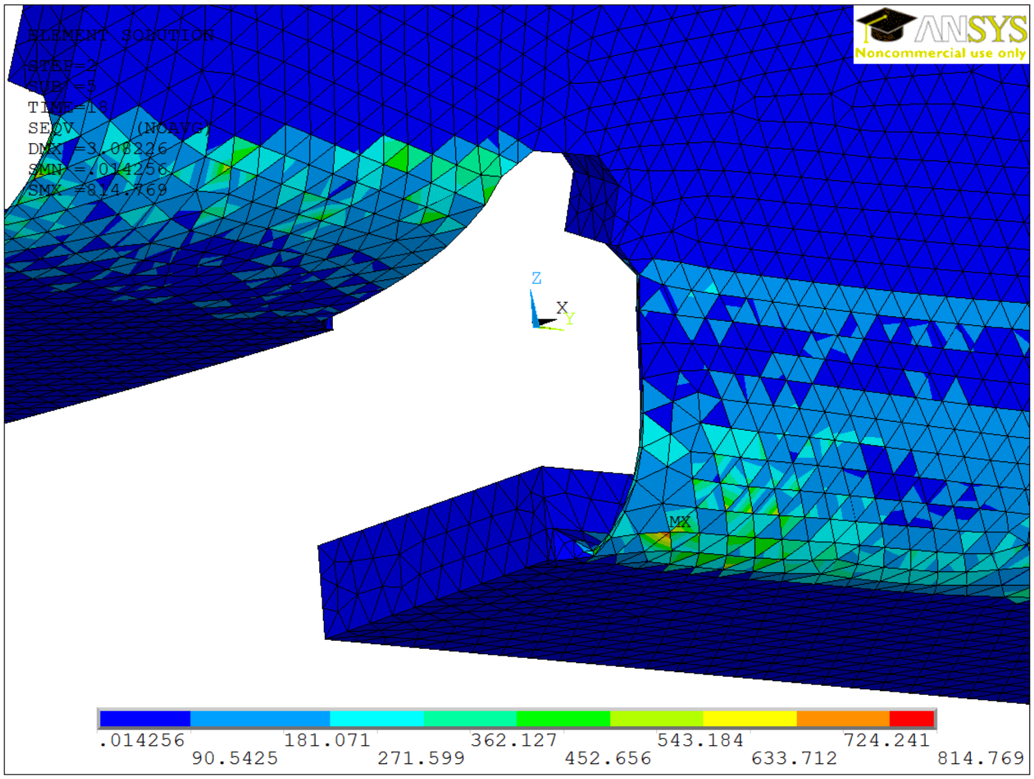

Figure 29. Von Mises Stress, Element Solution

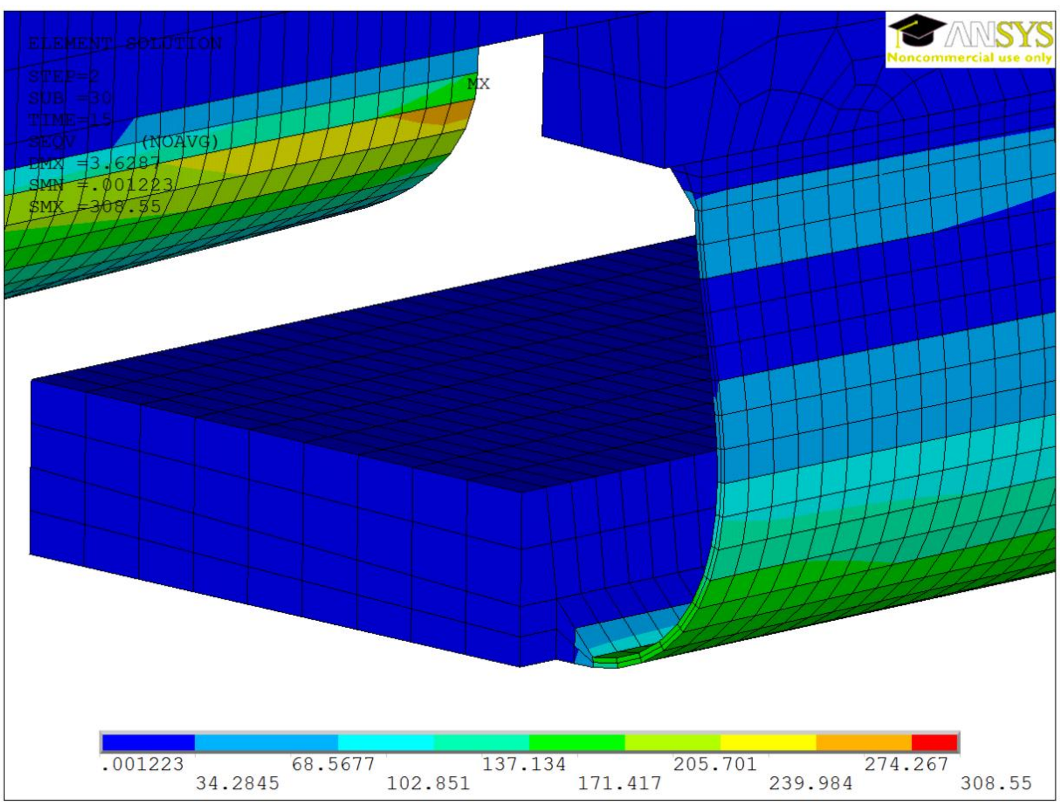

Figure 30. Von Mises Stress, Element Solution

Figure 31 shows a top and side view of the static displacement of the 3D Eristalis wing brick element model in comparison to the 2D beam model. In the 2D beam model it was assumed that all loads from the central flexure were transferred completely to the outer flexures. This picture shows that there is a small amount of bending in the rigid wing body section, but measuring this deformation in Ansys showed that the offset is less than 2 degrees.

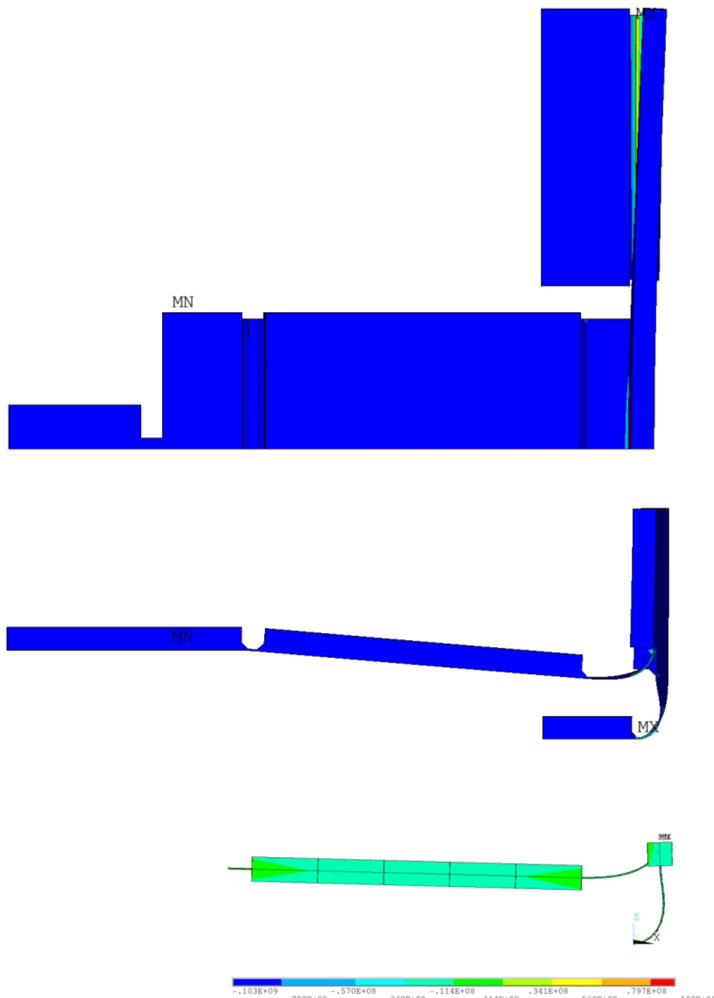

Figure 31. Model Comparison

LionFly 2.0 Model

A new design prototype utilizing a piezoelectric bimorph and compliant hinges has been proposed by Rahn and Tadigadapa [16]. However, this design has not been as extensively tested as the Eristalis design. The new design shows promise for the ability to amplify piezoelectric beam rotation into wing rotation while keeping the mechanism in a planar configuration.

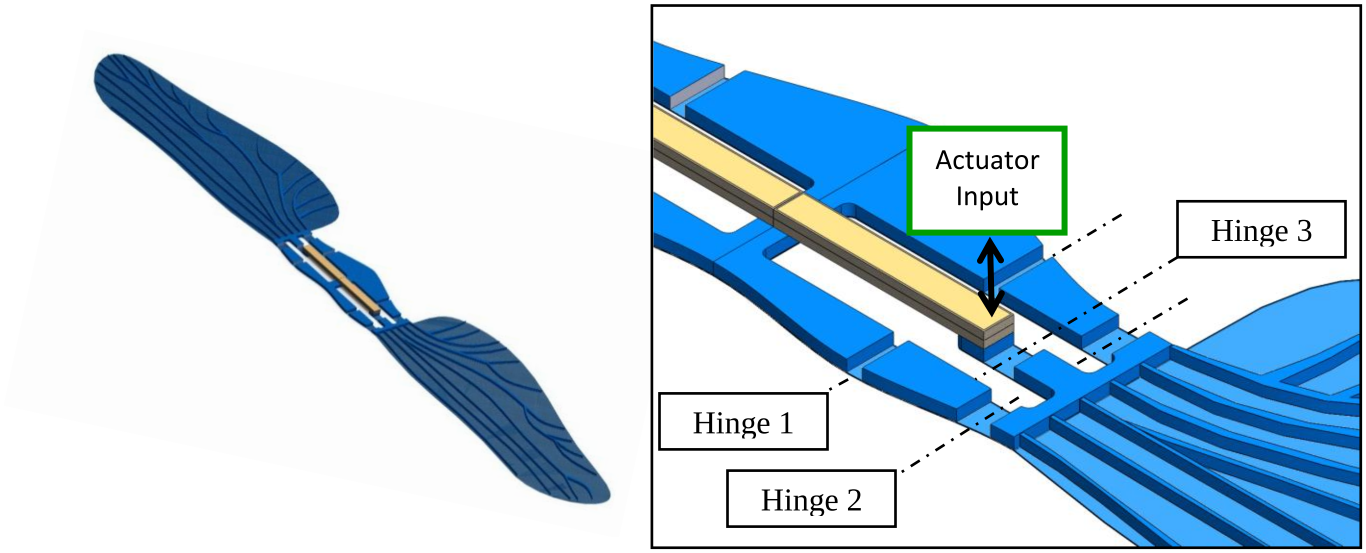

Figure 32. LionFly 2.0 Flapping Wing Model [16]

Model Creation

The LionFly 2.0 flapping wing mechanism in Figure 32 was modeled in Ansys 14.0 using the 2D Beam Element process developed for the Eristalis mechanism. The actual wing hinge dimensions were not given, but the model was created on the same scale as the Eristalis wing. The length of each flexure was set to 0.5 mm, and the width of each flexure was defined as 1 mm.

The Piezoelectric bimorph actuator was also included in the model and represented with beam elements. In this model, the Piezoelectric beam was only a single linear isotropic elastic material. It is expected that this is not an accurate representation of an actual Piezoelectric bimorph which is composed of three separate layers. However, the assumption was made for the bimorph, as other parts contributing to the stiffness of the LionFly 2.0 are still unknown. Specifically, the wing was only modeled as a single spar, when in actual operation the wing will include LionFly veins and other stiffening supports.

Static Analysis

First, a static analysis was run. The load for the static analysis was equal to the blocking force, 40 mN, of the piezoelectric bimorph used in the Eristalis Model [1]. Figure 33 shows the stresses in the model under this loading. The maximum stress appears in the bimorph itself, and not the flexure hinges of the mechanism. This is a promising sign, as under only the initial static displacement in the Eristalis wing, already large stresses were created in the flexure hinges.

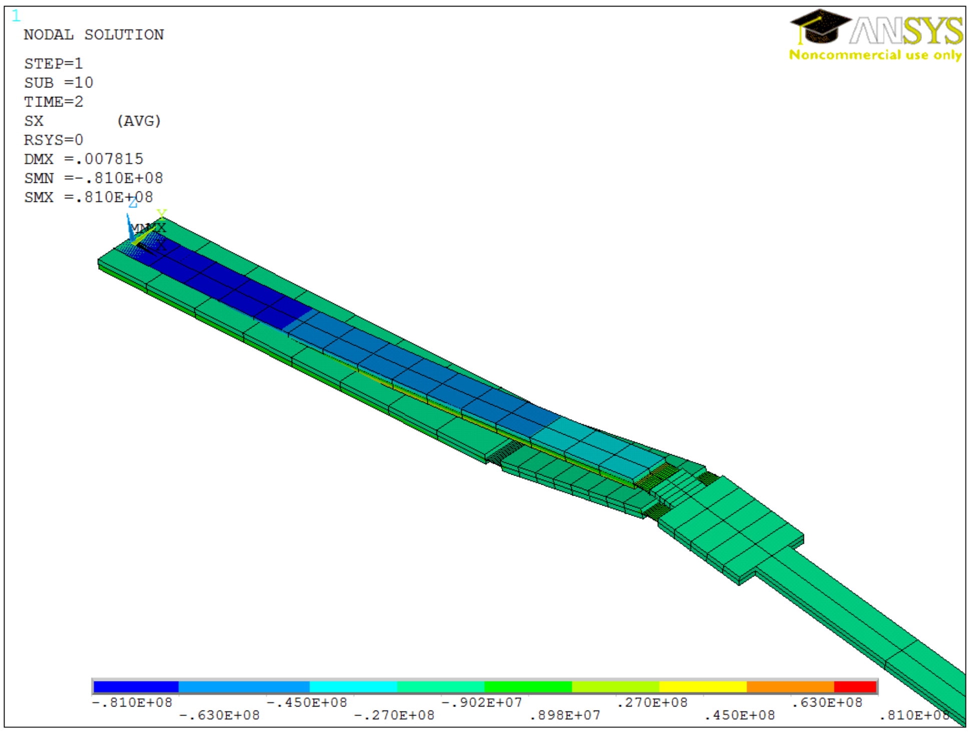

Figure 33. LionFly 2.0 Static Displacement

Harmonic Analysis

Another benefit of modeling the new LionFly 2.0 mechanism is that a harmonic analysis can be performed as the very first load step. The LionFly 2.0 model does not need to be displaced to some intital angle before applying an oscillating force, as in the Eristalis model. Therefore, a harmonic analysis is defined in Ansys. To carry out a harmonic analysis, the user must specify the desired frequency sweep range and number of substeps within the frequency range. A force load was again applied on the tip of the bimporh equal to the 40 mN force. The harmonic analysis then considers the force as the magnitude of a sinusoid wave and is able to solve for the resonance frequency of the model. After a few iterations with broad frequency ranges, it was discovered that the resonance frequency of the LionFly 2.0 is 3.4 Hz as seen below in Figure 34.

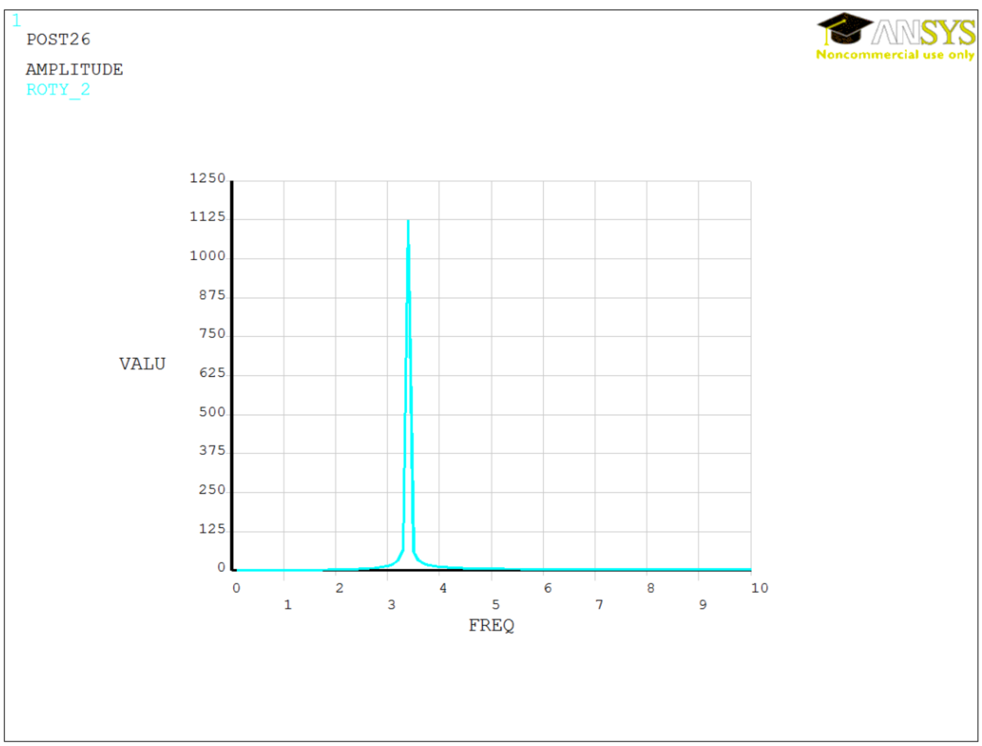

Figure 34. Frequency Response

Deformation or stress results can also be displayed for any of the substeps in the harmonic analysis. Figure 35 shows the harmonic response for the model at 3.6 Hz. It is not as useful to display the deformed structure at the exact resonant frequency, as it is highly deformed. The radian values plotted in Figure 35 show that the piezoelectric beam tip angle is amplified by a factor of approximately 15 to produce the wing rotation.

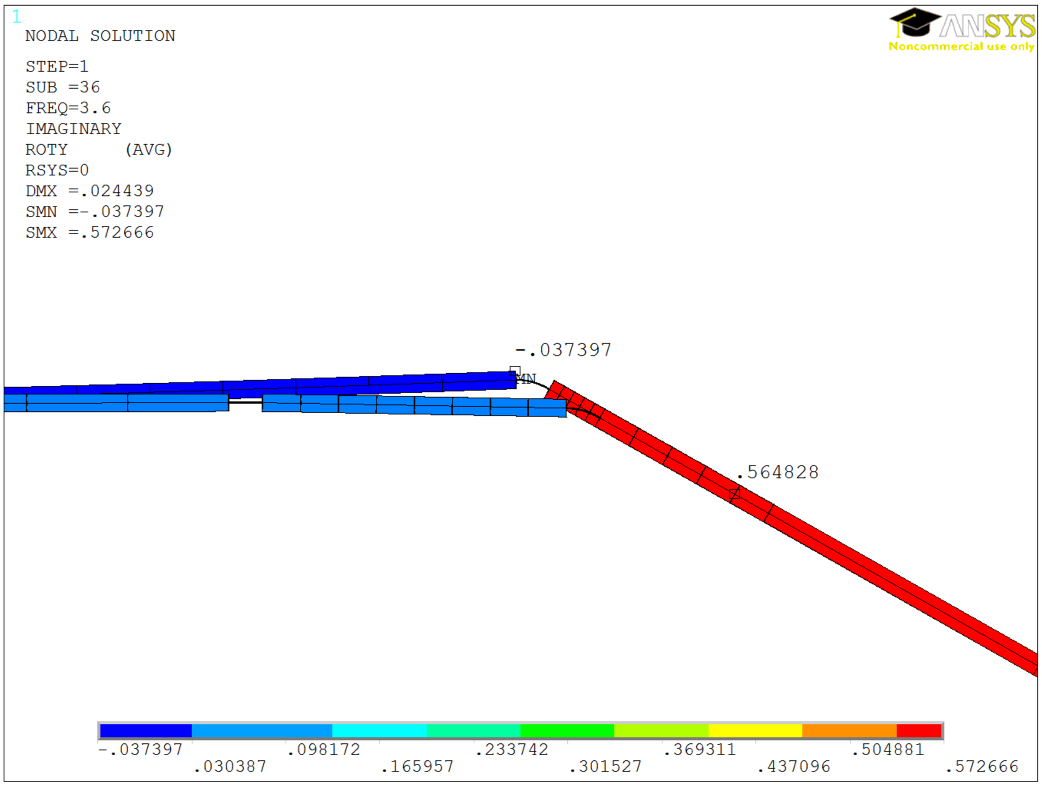

Figure 35. Rotation Plot (Radians) for a 40 mN Force at 3.6 Hz

Transient Analysis

Once the resonance frequency of the model has been determined, a 40 mN load applied sinusoidally at 3.6 Hz can help produce more detailed plots to display the amplification of the wing rotation. The ramped sinusoid force is defined as:

$$F_{actuator} = 0.04*((1 - \exp(-2*\{TIME\}))*\sin(2*\pi*3.6*\{TIME\}))$$

Figure 36 shows the angle in degrees of the wing spar in light blue and the angle of the bimorph tip in purple. This shows a much different result from the very large amplification predicted by the harmonic analyisis at 3.6 Hz. The curves plotted in figure 36 show that the piezoelectric beam tip angle is only amplified by a factor of approximately 2.0 to produce the wing rotation.

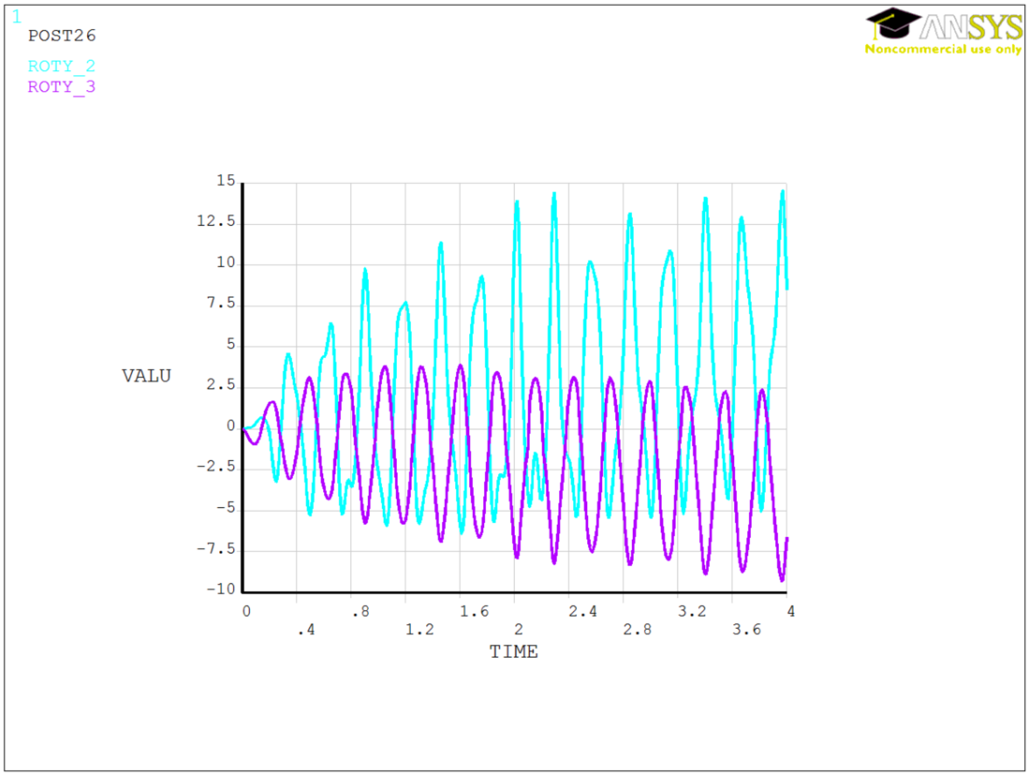

Figure 36. Rotation Amplification

The Harmonic Analysis and Transient Analysis provide significantly different amplification values for the operation of the LionFly 2.0 Model. The exact cause of this difference is unknown. However, it is believed that the mass and stiffness properties are handled differently within Ansys for the different solution types.

Conclusions

The theoretical, 2D, and 3D FEA models of the Eristalis flapping wing mechanism reveal that the yield stress of the SUEX material is exceeded under the current method of operation. Oscillating wing rotation about an initial angle of 77° constantly induces high bending stresses in the flexures. The LionFly 2.0 design represents an attractive solution to the high stresses that cause the Eristalis wing design to fail. The ability to create a significant flap angle from a planar configuration, with no initial angle requirement, may lead to a more robust flapping wing mechanism.

Model Comparisons

The 3D Eristalis wing model produces higher stresses in the flexure hinges than those stresses seen in the idealized 2D Eristalis model. At larger wing angles, out-of-plane twisting of the outer flexure hinges becomes significant, making the pure beam assumption of the 2D model less valid. Stress is also found to concentrate at the corner interface between the inner flexure and the wing body. This section experiences both a large bending deformation and a significant tensile stress as the piezoelectric forces it horizontally.

While producing lower stresses, the 2D beam model does accurately represent the rotation and displacement of the 3D model. The 2D model provides a valuable tool for quickly establishing a baseline stress level for a given flexure hinge design. The results of the 2D Ansys beam model also strongly match the large displacement and pseudo-rigid-body theoretical models.

Simpler finite element models are more useful in modeling the Eristalis and LionFly 2.0 flapping wing mechanisms. The operation of both wing mechanisms is by nature highly dynamic. Dynamic analysis in a complex model will be very CPU intensive with long run times. For example, the 2D beam model required only a 30 second run time as opposed to the 3D model, which required longer than a 30 minute run time. The high aspect ratio of the thin flexure hinges also necessitates a very high and burdensome number of elements to represent the geometry accurately with 3D elements for stress analysis purposes.

Addressing Limitations of the Finite Element Analysis Models

There are approximations made throughout the finite element modeling process. The surface roughness of the flexure hinges has been neglected, and in the models the surface is assumed to be smooth. The actual surface roughness of the flexure hinges after the photoresist etching process is unknown. Also, in the Eristalis model displacement of the piezoelectric pad is prescribed to be only in the +/- x direction. In reality displacement of the piezoelectric beam tip will include a very small +/-y component due to the rotation of the bimorph.

Under these several assumptions, the Finite Element Method may begin to approach an exact solution for the Eristalis flapping wing mechanism. But perhaps more importantly, it gives valuable information about the Eristalis wing operation and its potential for optimization. Nothing can replace the actual construction and experimental testing of the Eristalis and LionFly 2.0 mechanisms as the only true design test. Instead, the Finite Element Method can help approach an optimized flexure hinge design more quickly.

Appendix

Eristalis Wing Operating Pictures

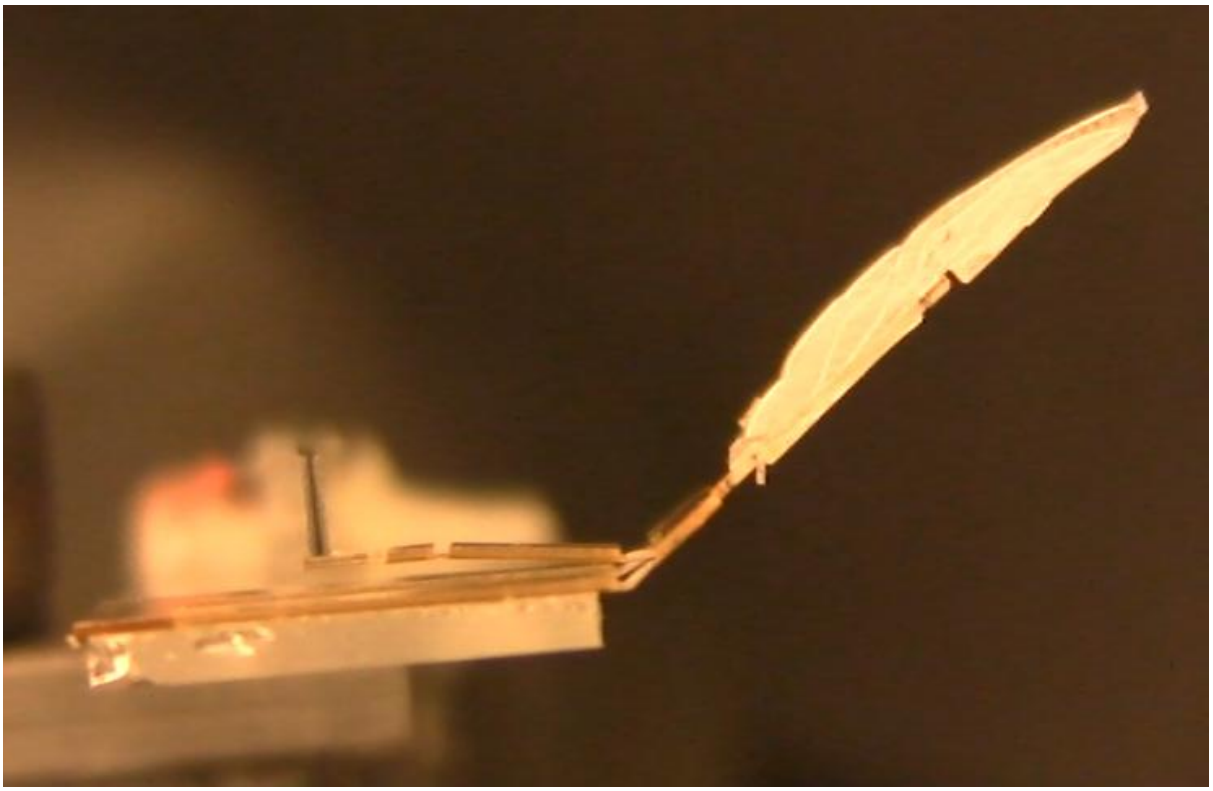

Figure 37. -150 V Static Displacement

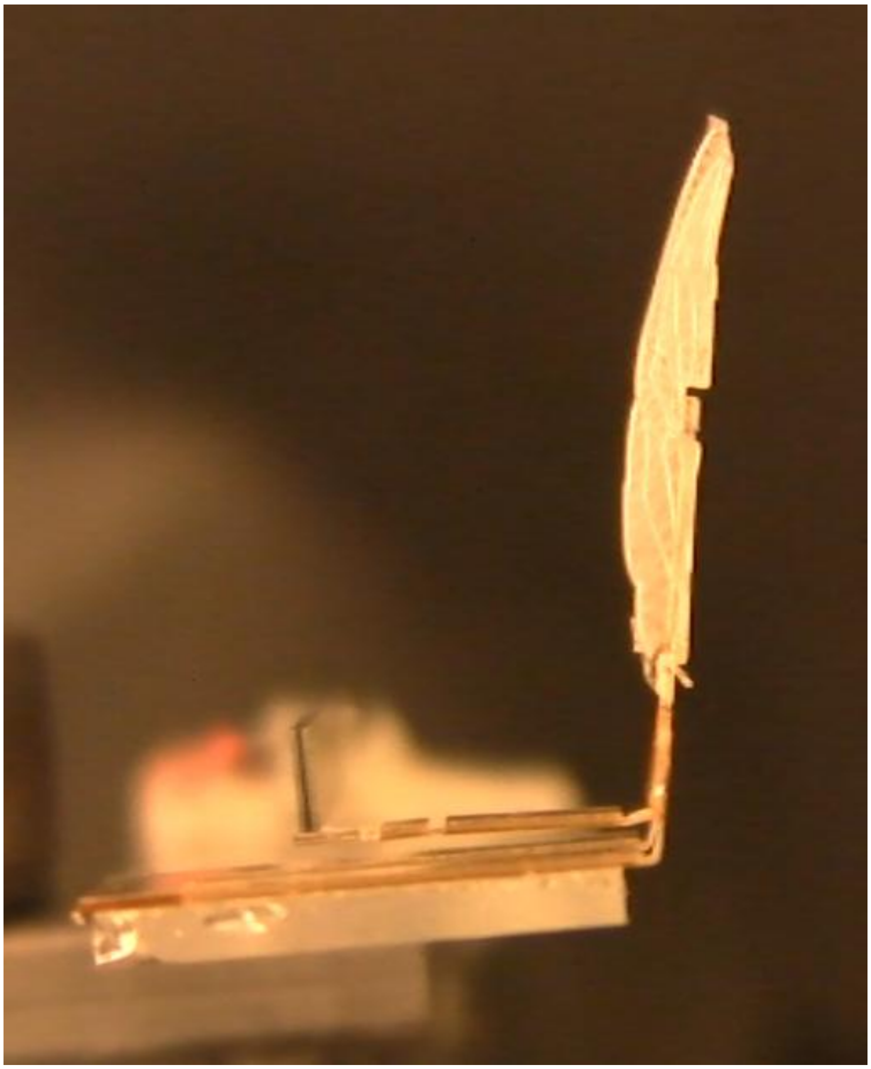

Figure 38. 0 V Static Displacement

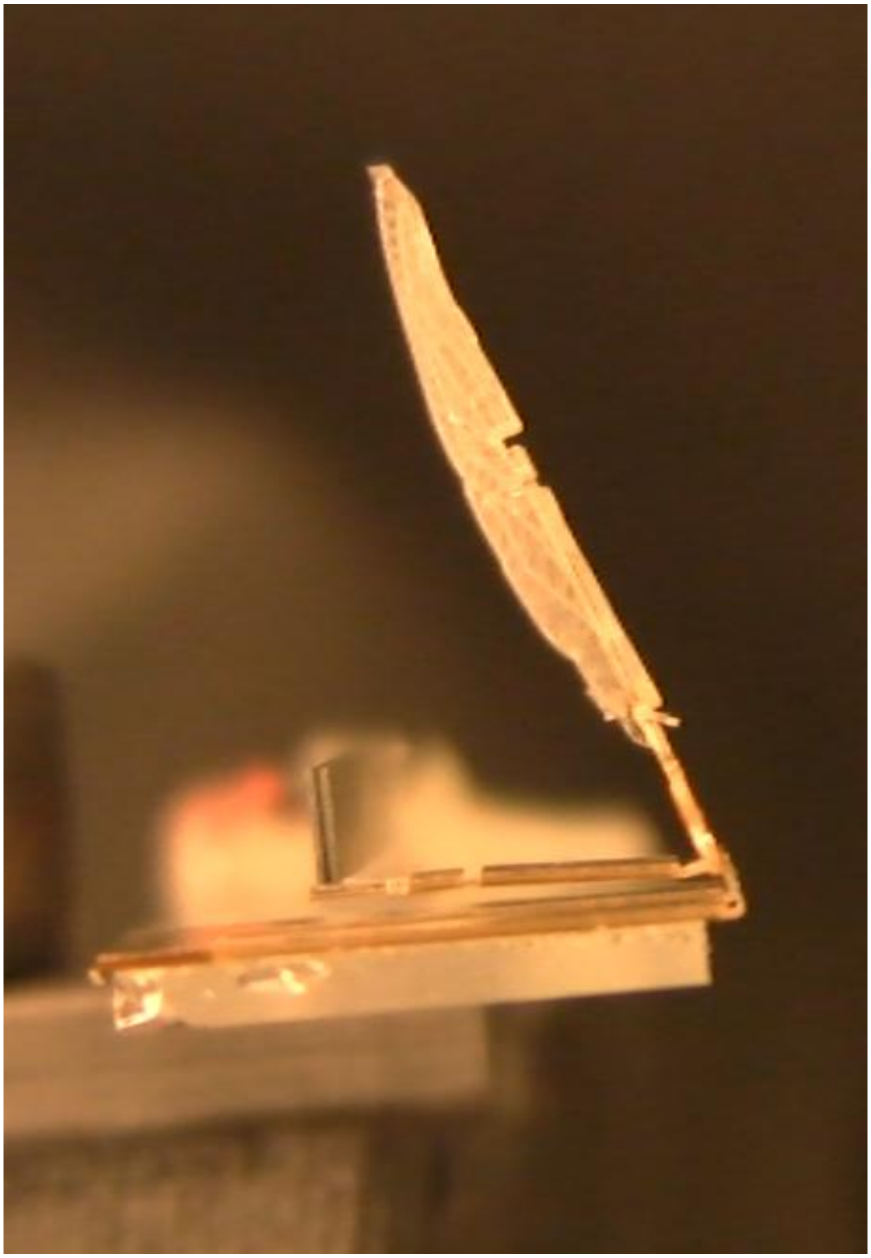

Figure 39. +150 V Static Displacement

References

[1] Mateti, Kiron. “Flapping Wing Mechanisms for Pico Air Vehicles Using Piezoelectric Actuators.” PhD dissertation, The Pennsylvania State University, 2012.

[2] Howell, L. L. *Compliant Mechanisms*. New York: John Wiley & Sons, Inc., 2001. Print.

[3] *SUEX Data*. DJ DevCorp. Web. 14 May 2012. <http://www.djdevcorp.com/15501.html>

[4] Tanaka, H., Whitney, J. P., and Wood, R. J. “Effect of Flexural and Torsional Wing Flexibility on Lift Generation in Hoverfly Flight” *Integrative and Comparative Biology* 51.1 (2011): 142-150. Web. 8 May 2012.

[5] Smith, Stuart T. *Flexures: Elements of Elastic Mechanisms*. Singapore: Gordon and Breach Science Publishers, 2000. Print.

[6] Raghavendra, M. R. A., Kumar, A. S., and Jagdish, B. N. “Design and analysis of flexure-hinge parameter in microgripper” *Int. J. Adv. Manuf. Technol.* 49 (2010):1185–1193. Web. 14 May 2012.

[7] Yong, Y. K. and Lu, T. F. “The effect of the accuracies of flexure hinge equations on the output compliances of planar micro-motion stages” *Mechanism and Machine Theory* 43 (2008): 347-363. Web. 21 March 2012.

[8] Beléndez, T., Neipp, C., and Beléndez, A. “Large and small deflections of a cantilever beam” *European Journal of Physics* 23.3 (2002): 371-379. Web. 25 September 2012.

[9] Johnstone, R. W., Ma, A. H., Sameoto, D., Parameswaran, M. and Leung, A. M. “Buckled cantilevers for out-of-plane platforms.” *J. Micromech. Microeng.* 18 (2008). Web. 28 September 2012.

[10] Timoshenko, S. P. and Gere, J. M. *Theory of Elastic Stability.* New York: McGraw-Hill, 1961. Print.

[11] Zettl, B., Szyszkowski, W., and Zhang, W. J. "Accurate low DOF modeling of a planar compliant mechanism with flexure hinges: the equivalent beam methodology" *Precision Engineering* 29 (2005): 237-245. Web. 3 March 2012.

[12] ANSYS Users Guide. Release 14.0. Copyright 2011 SAS IP, Inc.

[13] Logan, D. L. *A First Course in the Finite Element Method*. Toronto: Nelson, 2007. Print.

[14] Johnson, David. *MET 415/425 Lecture Notes: Postprocessing BEAM & TRUSS.* The Pennsylvania State University. Web. 10 October 2012. <http://engr.bd.psu.edu/davej/classes/lec_ppbeams.html>

[15] SolidWorks Users Guide. 2012-2013 Education Edition. Copyright 1995-2012 Dassault Systèmes.

[16] Rahn, C. D. and Tadigadapa, S. "Heterogeneous Integration of Piezoelectric and Polymer Materials for NAV Structures." Proposal Concept. PowerPoint. 10 October 2012.

ACADEMIC VITA

Peter Alan Koffler
pak5110@psu.edu

Education
B.S., Mechanical Engineering, December 2012
The Pennsylvania State University, University Park, PA

Honors and Awards
Louis Harding Memorial Scholarship, 2012-2013 Academic Year
Louis Harding Memorial Scholarship, 2011-2012 Academic Year
Schreyer Ambassador Travel Grant, May 2011
Penn State Annapolis Area Alumni Association Scholarship
The President's Freshman Award, December 2009
Northrop Grumman Engineering Scholarship, June 2009
Eagle Scout, Boy Scouts of America, June 2009

Association Memberships/Activities
Tau Beta Pi Engineering Honor Society

Professional Experience
NASA Wallops Flight Facility — Wallops Island, VA — June – August, 2012
Airworthiness Engineering Intern
- Designed a mounting structure for two air-sampling probes using Autodesk Inventor
- Analyzed stresses using Femap and NX Nastran after calculating aerodynamic and inertial load cases based on flight conditions
- Served as an interface between pilots, scientists, engineers, and mechanics to assist in the mission management of a series of flights at Dryden Flight Research Center

Academic Excellence Center — University Park, PA — August 2011 – May 2012
Undergraduate Engineering Tutor
- Helped students to study for introductory math, physics, and engineering mechanics classes for 10 hours per week

Albert-Ludwigs-Universität — Freiburg, Germany — June – August, 2011
Undergraduate Research Intern, DAAD RISE Program
- Designed and laser-machined multiple electromagnetic vibrational energy harvesters using Solidworks and a Trumph TruMark marking laser for a German PhD student
- Assembled and tested the different varieties of 2 cm^3 harvesters on a shaker machine to compare the effectiveness of different spring-mass systems for energy harvesting

The KEYW Corporation — Severn, MD — June – August, 2010
Engineering Intern
- Created 3-D graphic models and engineering drawings using SolidWorks
- Performed assembly, integration, and testing processes for SMT microelectronics